Streptococcus pneumoniae drives specific and lasting Natural Killer cell memory

Tiphaine M.N. Camarasa, Júlia Torné, Christine Chevalier, Orhan Rasid, Melanie Anne Hamon

Title: *Streptococcus pneumoniae* drives specific and lasting Natural Killer cell memory

Authors: Tiphaine M.N. Camarasa[1,2], Júlia Torné[1], Christine Chevalier[1], Orhan Rasid[1,3], Melanie Anne Hamon[1,*]

[1] Chromatin and Infection Unit, Institut Pasteur, Paris, France

[2] Université Paris Cité, 562 Bio Sorbonne Paris Cité, Paris, France

[3]Present address: School of Infection and Immunity, University of Glasgow, Glasgow, United Kingdom.

[*] correspondence: melanie.hamon@pasteur.fr

Abstract

NK cells are important mediators of innate immunity and play an essential role for host protection against infection, although their responses to bacteria are poorly understood. Recently NK cells were shown to display memory properties, as characterized by an epigenetic signature leading to a stronger secondary response. Although NK cell memory could be a promising mechanism to fight against infection, it has not been described upon bacterial infection. Here, we reveal that NK cells develop specific and long-term memory following sub-lethal infection with the extracellular pathogen *Streptococcus pneumoniae*. Memory NK cells display intrinsic sensing and response to bacteria *in vitro*, in a manner that is enhanced post-bacterial infection. In addition, their transfer into naïve mice confer protection from lethal infection for at least 12 weeks. Interestingly, NK cells display enhanced cytotoxic molecule production upon secondary stimulation and their protective role is dependent on Perforin and

independent of IFNγ. Thus, our study identifies a new role for NK cells during bacterial infection, opening the possibility to harness innate immune memory for therapeutic purposes.

Introduction

In the last decade, the discovery of memory responses mediated by innate immune cells has questioned the dogma that only adaptive immune cells retain memory of previous exposure. Monocytes and macrophages have been shown to acquire an innate immune memory described by a faster and greater response against a secondary challenge with homologous or even heterologous pathogens (Divangahi et al. 2021; Hamon and Quintin 2016). This capacity, termed trained immunity, is defined by a return to basal state of activation after removal of the primary stimulus, accompanied by the acquisition of persistent epigenetic changes and metabolic rewiring necessary for enhanced response to secondary challenge (Saeed et al., 2014; Quintin et al., 2014).

Natural Killer (NK) cells also display memory properties, which are different from those of macrophages and monocytes. Indeed, memory NK cells display high antigen-specificity and undergo clonal expansion of specific receptor-defined sub-populations (Cerwenka and Lanier 2016; Geary and Sun 2017; O'Sullivan, Sun, and Lanier 2015). NK cell memory has been well studied in the context of viral infections (CMV, Epstein-Barr virus, etc.), however, evidence of memory following bacterial infection, especially extracellular bacteria, remains undefined (Sun, Beilke, and Lanier 2009; Lopez-Vergès et al. 2011; Azzi et al. 2014; Littwitz-Salomon et al. 2018; Wijaya et al. 2021). In fact, the role of NK cells during bacterial infections is controversial (Theresine, Patil, and Zimmer 2020). IFNγ produced by NK cells, contributes to bacterial clearance by activating immune cells, such as macrophages and neutrophils to enhance phagocytosis in the case of lung infections with *L. pneumophila*, *K. pneumoniae* or *M.*

tuberculosis among others (Spörri et al., 2006; Ivin et al., 2017; Feng et al., 2006). However, upon infection with bacillus Calmette-Guérin (BCG), *S. pneumoniae* or *S. pyogenes*, NK cells can be deleterious, leading to tissue damage associated with an excessive inflammatory response (Wang et al. 2018; Kerr et al. 2005; Christaki et al. 2015; Goldmann, Chhatwal, and Medina 2005). In addition, although some studies show that NK cells induce apoptosis of infected cells (Dornand et al. 2004; Voskoboinik, Whisstock, and Trapani 2015; Gonzales et al. 2012), others find that certain intracellular bacterial infections are not affected by NK cells (Fernandes, Benson, and Baldwin 1995; Junqueira-Kipnis et al. 2003).

Streptococcus pneumoniae (also known as pneumococcus) is a Gram-positive, extracellular bacterium and natural colonizer of the human upper respiratory tract but also an opportunistic pathogen (Weiser, Ferreira, and Paton 2018). Indeed, although *S. pneumoniae* resides asymptomatically in its natural reservoir, the nasopharynx, it can spread to the lungs or enter the bloodstream causing deadly invasive inflammatory diseases such as pneumonia, meningitis and sepsis (Kadioglu et al., 2008; Bogaert, de Groot, and Hermans 2004; Gillespie and Balakrishnan 2000). Comparable to other bacterial infections, the role of NK cells during *S. pneumoniae* infection is poorly understood. NK cells contribute to infection clearance by IFNγ production in the lungs (Baranek et al., 2017), however, NK cell production of IL-10 is detrimental to infected mice (Clark et al. 2020).

In this study, we used *S. pneumoniae* to explore NK cell responses to an extracellular bacterial infection. We show that NK cells directly sense and respond to *S. pneumoniae*, as well as acquire memory properties. Upon clearance of a primary infection, NK cells retain intrinsic heightened *in vitro* response to *S. pneumoniae*, and *in vivo* they acquire protective functions against lethal infection. Interestingly, we demonstrate that NK cell protection is mediated through higher levels of cytotoxic products (Granzyme B and Perforin), and not through IFNγ

mediated responses or inflammatory cell recruitment, thereby revealing a novel role for NK cells in bacterial infection.

Results

NK cells acquire intrinsic memory features 21 days after *in vivo* infection

We set up model in which mice were infected intranasally with a sub-lethal dose of *S. pneumoniae* (SPN, 5.10^5 CFU) or treated with PBS (Figure 1A). 21 days later, to test their intrinsic features, NK cells from the spleen were extracted, highly purified by negative selection (~98%, Figure S1A), and stimulated *ex vivo*. Naïve (D21PBS NKs) or previously exposed NK cells (D21SPN NKs) were incubated for 24 hours with different combinations of cytokines and/or formaldehyde inactivated SPN (Figure 1B). Upon incubation of NK cells with either medium alone, SPN alone, or IL-15+IL-18 (to ensure maintenance of cell viability), no production of IFNγ was detected. In contrast, IL-12+IL-18 (activating cytokines) activated both D21PBS and D21SPN NK cells to the same levels. These results show that under these *in vitro* conditions NK cells can be reproducibly activated. Strikingly, upon incubation with IL-15+IL-18+SPN, D21SPN NK cells displayed significantly higher signal per cell (MFI) and percentages of IFNγ^+ cells compared with control D21PBS NK cells (Figure 1B). These results indicate that memory IFNγ^+ NK cells are both more numerous and express IFNγ to higher levels upon secondary stimulation. Since the higher response of these cells occurs only under condition where bacteria are present with IL-15+IL-18, we can rule out that D21SPN NK cells are hyperactivated under any condition and are specifically responding to SPN. Therefore, NK cells from infected mice acquire intrinsic memory features which are detected *ex vivo* and

characterized by sensing *S. pneumoniae* and responding more strongly upon secondary stimulation compared to primo-stimulation.

Innate immune memory in macrophages, monocytes and NK cells has been described to correlate with chromatin modifications in various models (Lau, Wiedmann, and Sun 2022; Saeed et al., 2014). In particular, we have previously shown in Rasid et al., 2019 that NK cell memory in a post-endotoxemia model relies on H3K4me1 histone modification at an *ifng* enhancer. To explore whether this might be the case for NK cell memory to *S. pneumoniae*, we assessed the histone mark H3K4me1 associated with upstream regulatory regions of *ifng* gene in D21PBS and D21SPN NK cells by chromatin immunoprecipitation followed by qPCR (ChIP-qPCR). Interestingly, although we did not reach statistical significance, we always observed the same consistent increase of H3K4me1 at the *ifng* enhancer located at -22 kb in memory NK cells compared to naïve cells (Figure S1B). By contrast, we did not observe a difference in H3K4me1 at the -55 kb enhancer, suggesting histone modifications are occurring at specific regulatory loci. In addition, the increase of H3K4me1 we observed in D21SPN NK cells was located at the same region (-22 kb) than post-endotoxemia memory NK cells. Together, these data suggest that NK cell memory is associated with epigenetic changes at upstream regulatory regions of *ifng* gene.

The Ly49H, NKG2C and NKG2A receptors have been shown to be implicated in NK cell recognition and memory responses to MCMV, HCMV and EBV respectively, leading to an expression increase upon infection (Sun, Beilke, and Lanier 2009; Lopez-Vergès et al., 2011; Azzi et al., 2014). We tested the expression levels of several NK cell receptors in post-SPN NK cells. As early as 12 days post-infection, we observe no difference in the percentage of NKG2D, Ly49D, Ly49H, or Ly49F positive cells between D12PBS and D12SPN NK cells. A small increase in the percentage of Ly49C/I^{+} NK cells is observed, which was no longer detectable 21 days post-infection (Figure S1C-D). Therefore, although NK cells acquire memory

123 properties post-bacterial infection, none of the known NK cell receptors previously associated
124 with memory NK cells seem to be involved.
125
126 **Sub-lethal infection with *S. pneumoniae* induces a rapid and transient immune response**
127 **that returns to basal state before 21 days.**
128
129 To understand the immune environment from which NK cells were extracted, we
130 studied a primary infection. Mice were infected as described Figure 1A, and organs were
131 collected at 24 hours, 72 hours and 21 days post-infection (Figure 2A). Using this infection
132 protocol, mice displayed no weight loss and showed minimal clinical signs (Figure S2A-B). At
133 24 hours, bacteria were mostly located in the nasal cavity (Figure 2B) and spread into bronchio-
134 alveolar lavage fluid (BALF) and lungs at 72 hours post-infection (Figure 2C). Importantly, no
135 dissemination was observed following this dose of infection, as demonstrated by the
136 undetectable levels of bacteria in the blood and spleen at both 24 and 72 hours (Figure 2B-C).
137 The sub-lethal infection that we perform is accompanied by a low-level immune
138 response. Indeed, at 24 hours, an increase in the percentage and number of neutrophils in the
139 lungs and BALF was detectable, but rapidly decreased to basal levels at 72 hours (Figure 2B-
140 C, numbers in S2C-D). Furthermore, a small increase of $CD69^+$ neutrophils was detected in the
141 BALF at 72 hours, suggesting a low level of activation of these cells (Figure 2C). In contrast to
142 neutrophils, we did not detect an increase in NK cell percentages or numbers in the lungs at any
143 time point (Figure 2B-C, numbers in S2C-D). In addition, we tested responsiveness of NK cells
144 by measuring IFNγ, CD69, Perforin and Granzyme B expression. A small increase in IFNγ^+
145 and $CD69^+$ NK cells was observed in the lungs only at 24 hours and 72 hours respectively
146 (Figure 2B and S2D), but no increase of $Perforin^+$ and Granzyme B^+ cells was detected at both
147 24 and 72 hours post-infection (Figure 2B-C, MFI in S2C-D). Together these data indicate that

148 sub-lethal infection with SPN induces a low, rapid and transient immune response characterized
149 by the recruitment of neutrophils but no significant NK cell responses.

150 To study the inflammatory environment at 21 days post-infection, we harvested organs
151 and performed bacterial enumeration. At this time point, no bacteria were recovered in the nasal
152 lavage, BALF, lungs, or spleen (Figure 2D), demonstrating that bacteria had completely been
153 cleared. Additionally, the immune parameters returned to pre-infection state as the percentage
154 and number of neutrophils and NK cells detected in 21 days infected mice was the same as in
155 control PBS mice (Figure 2D, numbers in S2E). Similarly, both neutrophils and NK cells
156 showed no sign of activation in the BALF, lungs and spleen respectively (Figure 2D and S2E).
157 Therefore 21 days after primary exposure, infection by *S. pneumoniae* is no longer detected and
158 immune cells are similar to uninfected conditions, both in their number and activity.
159

160 **Transferred memory NK cells protect mice from lethal *S. pneumoniae* infection for at**
161 **least 12 weeks**
162

163 As NK cells display intrinsic sensing and memory activities *in vitro*, we investigated the
164 potential role of D21SPN NK cells during lethal *S. pneumoniae* challenge *in vivo*. We
165 adoptively transferred purified D21PBS or D21SPN NK cells into naïve mice (2.10^5 cells,
166 intravenously, Figure 3A) and one day after the transfer, recipient mice were intranasally
167 infected with a lethal dose of SPN (1.10^7 CFU). At all times points, transferred congenic
168 $CD45.2^+$ NK cells were circulating and detectable at similar percentages in lungs and blood,
169 suggesting there is no preferential trafficking between D21PBS and D21SPN NK cells (Figure
170 S3A-B). Importantly, we observed a significant reduction in bacterial counts at 40 hours in all
171 tested organs of mice having received D21SPN NK cells compared with those having received
172 D21PBS NK cells, which is not observed at 24 hours (Figure 3B). Additionally, the transfer of

D21SPN NK cells reduced mortality and clinical signs in recipient mice infected with *S. pneumoniae* (5.10^6 CFU, Figure 3C-D). We observed a 75% survival rate for mice having received D21SPN NK cells compared to only 25% for those having received D21PBS NK cells. Interestingly, both groups of mice lost similar weight during the first days of infection (Figure 3E). Thus, our results demonstrate that the transfer of as few as 2.10^5 D21SPN NK cells confers protection compared to D21PBS NK cells during lethal *S. pneumoniae* infection.

To evaluate long term protection, we purified naïve or memory NK cells 12 weeks after primary exposure (W12PBS or W12SPN) and transferred them prior to lethal infection with *S. pneumoniae*. Remarkably, we observed a similar significant reduction in bacterial counts in the lungs and spleen of mice having received W12SPN NK cells, as cells from 21 days post-primary exposure (Figure 3F). Therefore, NK cells retain memory of a primo *S. pneumoniae* infection, and maintain the ability to protect against lethal challenge, for at least 12 weeks.

To assess the specificity of the observed memory properties, we performed the same transfer model as described in Figure 3A, and infected recipient mice with a lethal dose of the heterologous bacterium *Listeria monocytogenes* (1.10^6 CFU, intravenously). Organs were collected 40 hours post-infection for bacterial enumeration (Figure 3G). Our results showed no differences in bacterial counts in the spleen of infected mice between the two conditions. Surprisingly we counted higher numbers of bacteria in the liver of mice having received D21SPN NK cells than D21PBS NK cells. Thus, *in vivo*, *S. pneumoniae* memory NK cells are not able to protect recipient mice from *L. monocytogenes* infection, demonstrating a specificity in their response to *S. pneumoniae*. Together, these data show that memory NK cells protect mice upon secondary *in vivo* infection, with specific and long-term properties.

Protection of mice mediated by memory NK cells is IFNγ independent

198 Because D21SPN NK cells showed higher expression of IFNγ upon secondary
199 stimulation *in vitro* (Figure 1B), we hypothesized that IFNγ production by memory NK cells
200 *in vivo* could be an important factor for protecting mice against lethal infection. Using CD45.1
201 and CD45.2 congenic mice, we compared intracellular IFNγ expression between transferred
202 and endogenous NK cells in both groups of mice receiving D21PBS or D21SPN NK cells
203 (Figure 4A). Upon lethal infection with SPN, IFNγ expression by NK cells increased at 40
204 hours in the lungs at equal levels between endogenous and transferred cells in the same mouse.
205 But surprisingly, both endogenous and transferred NK cells in mice receiving D21SPN NK
206 cells expressed lower levels of IFNγ than those having received D21PBS NK cells. In addition,
207 total lung IFNγ levels showed no difference between protected mice and control mice (Figure
208 4B). Therefore, memory NK cells are not producing more IFNγ upon secondary stimulation *in*
209 *vivo*.

210 To further address the role of IFNγ in protection, we transferred WT naive or WT
211 memory NK cells into IFNγ receptor deficient mice (Ifngr KO, Figure 4C). One day after the
212 transfer, we infected Ifngr KO recipient mice with the same lethal dose of SPN as in Figure 3A
213 and collected organs at 40 hours post-infection. By comparing both WT and Ifngr KO mice
214 having received naïve NK cells we did not detect significant differences in bacterial counts,
215 recruitment of neutrophils or activation of NK cells in the lungs at 40 hours (Figure 4D). These
216 results suggest that IFNγ signaling is not protective during early times of SPN infection.
217 Importantly, we still found a reduction in bacterial numbers in the spleen and lungs of Ifngr KO
218 recipient mice having received WT D21SPN NK cells compared to Ifngr KO recipient mice
219 having received WT D21PBS NK cells (Figure 4C). Strikingly, these data suggest that IFNγ
220 signaling is not necessary for the protection of mice having received memory NK cells.
221

222 **Protection of mice appears to be an intrinsic NK cell property**

To assess the protective functions of memory NK cells, we analyzed the innate immune response in the lungs of recipient mice. Using the transfer model described in Figure 3A, we infected recipient mice with a lethal dose of *S. pneumoniae* (1.10^7 CFU) and collected organs at 24 and 40 hours post-infection. With this infection protocol, bacteria are detectable in the BALF and lungs and disseminate to the bloodstream and spleen by 24 hours (Figure 3B). We first compared innate immune cell recruitment in the lungs and BALF of infected mice having received naïve or memory NK cells (Figure 5A-B, full gating strategy in Figure S4A). Although we observed a robust recruitment of neutrophils at 24 hours in the lungs and BALF of infected mice, we found similar percentages and numbers of neutrophils between the two groups of recipient mice. We observed the same reduction in the percentages and numbers of alveolar macrophages in the lungs and BALF of infected mice having received either naive or memory NK cells. Surprisingly, we do not observe a significant recruitment or increase in other innate immune cell types (interstitial macrophages, eosinophils, dendritic cells, monocytes or NK cells) in the lungs of either group of infected mice compared to uninfected.

We next evaluated innate immune cell activation in the lungs of recipient mice at 40 hours post-infection. Although neutrophils and NK cells upregulated CD69 compared to uninfected animals, we did not detect any difference between mice having received naïve or memory NK cells (Figure 5C). Additionally, in neutrophils, we did not observe an increase in the intensity of CD11b expression (MFI) or in the percentage of ROS^+ cells compared to uninfected cells (Figure S4B). Furthermore, interstitial macrophages had the same values of $CD86^+$ cells and intensity of MHCII expression between mice having received D21PBS or D21SPN NK cells (Figure 5C and S4B). Therefore, alongside no differential innate immune cell recruitment, we did not detect an increase in immune cell activation in the lungs of

247 protected mice. These results indicate that the protection provided by memory NK cells is not
248 through enhanced recruitment or activation of inflammatory cells.

249 To further investigate the mechanisms of protection mediated by memory NK cells, we
250 quantified selected cytokines and chemokines in lung supernatants by ELISA (Figure 5D at 40
251 hours, Figure S4C at 24 hours). Coherent with our observation that innate immune cells are not
252 recruited and activated to higher levels by memory NK cells, we did not detect an increase of
253 pro-inflammatory cytokines in the lungs of mice having received D21SPN NK cells. In fact,
254 we showed a signification reduction of CXCL1 production in the lungs of protected mice
255 (Figure 5D).

256 In addition to cytokines/chemokines signaling, we also studied release of cytotoxic
257 molecules *in vivo* by comparing Granzyme B production in the lungs of infected mice having
258 previously received D21PBS or D21SPN NK cells (scheme in Figure 3A). Importantly, ELISA
259 on lung supernatants showed an increase of Granzyme B at 40 hours post-infection in mice
260 having received D21SPN NK cells compared to control (Figure 5E), which was not observed
261 at 24 hours post-infection (Figure S4D). Interestingly, the decrease in bacterial numbers in mice
262 having received D21SPN NK cells is detectable at 40h, not at 24h (Figure 3B). Furthermore,
263 we also found the same increase of Granzyme B production in the lungs of mice having received
264 long term memory NK cells (We12SPN NKs, Figure 5F). Therefore, transferring memory NK
265 cells induced a greater production of Granzyme B in the lungs of infected mice. Thus, our
266 results open the possibility that cytotoxic functions of memory NK cells could be important for
267 the protection of mice upon secondary lethal *S. pneumoniae* infection.

268

269 **Cytotoxic proteins are upregulated by memory NK cells and important for protection of**
270 **mice**

271

To further investigate an upregulation of cytotoxic proteins by memory NK cells, we stimulated purified naïve and memory NK cells *in vitro* with inactivated *S. pneumoniae.* Interestingly, cytokines alone did not induce Granzyme B or Perforin expression in either naïve or memory NK cells (Figure 6A-B). However, addition of SPN stimulated Granzyme B and Perforin expression specifically in memory NK cells. Indeed, an increase in both percentage of positive cells and intensity of expression was detected under this condition (Figure 6A-B). However, the incubation of memory NK cells with inactivated *L. monocytogenes* or *Streptococcus agalactiae* (GBS) did not induce an increase of Granzyme B and Perforin (Figure 6A-B), supporting once again the specificity of the response. Therefore, NK cells respond to and remember SPN in an intrinsic and specific manner, by releasing cytotoxic proteins.

To explore whether heightened cytotoxic function of memory NK cells is associated with epigenetic changes, we assessed the histone mark H3K4me1 associated with upstream regulatory regions of *gzmb* gene in D21PBS and D21SPN NK cells. Although we did not reach statistical significance, we showed a consistent increase of H3K4me1 at -34kb upstream *gzmb* gene in D21SPN NK cells compared to D21PBS NK cells (Figure S5A), which was not observed at the intergenic region (IG). Thus, our results suggest that memory NK cells are associated with a gain of H3K4me1 at specific regulatory loci of *gzmb* gene.

To analyze the role of cytotoxic proteins in the protection of mice, we used Perforin KO mice. First, we generated D21PBS or D21SPN Perforin KO NK cells as previously described in Figure 3A. To control that Perforin KO NK cells are still able to acquire memory properties upon *S. pneumoniae* infection, we stimulated them *in vitro* and showed that D21SPN Perforin KO NK cells produce more Granzyme B than D21PBS Perforin KO NK cells upon stimulation with IL-15+IL-18+SPN (Figure S5B). Next, we transferred highly purified naïve or memory Perforin KO NK cells into naïve Perforin KO recipient mice and infected them with a lethal dose of *S. pneumoniae* (scheme in Figure 3A). Coherent with our *in vitro* results, we also

297 observed an increased production of Granzyme B in the lungs of mice having received D21SPN
298 Perforin KO NK cells compared to the control group (Figure S5C). In addition, we evaluated
299 the percentages of neutrophils and NK cells in Perforin KO mice and observed a similar
300 recruitment and activation of cells in both groups of recipient mice (Figure S5D). Importantly,
301 by comparing bacterial counts in the organs of recipient mice we do not observe a reduction of
302 CFU in mice having received D21SPN Perforin KO NK cells compared to control group
303 (Figure 6C). Therefore, our data suggest that protection of mice mediated by memory NK cells
304 is abolished in the absence of Perforin production.
305
306 **Discussion**
307
308 In this study, we show that NK cells play an important role in extracellular bacterial
309 infections, a property previously poorly described. Notably, NK cells retain an intrinsic memory
310 of previous bacterial encounters and display heightened responses upon secondary exposure to
311 the same bacterium and protect naïve mice from a lethal infection. Surprisingly, protection does
312 not require IFNγ or recruitment of inflammatory cells, instead, an inherent property of NK cells
313 and production of cytotoxic factors seem to be required.
314 Although NK cell memory has been described upon various viral infections, such
315 response to bacterial infections remains poorly understood. Upon infection with *Ehrlichia*
316 *muris*, an intracellular bacterial pathogen, Habib et al., 2016 suggested that NK cells develop
317 memory-like responses. Indeed, transferred memory-like NK cells from *E. muris*-primed donor
318 mice conferred protection in $Rag2^{-/-}$ $IL2rg2^{-/-}$ recipient mice against a high dose *E. muris*
319 challenge. However, these memory-like NK cells were not characterized and the mechanisms
320 involved in the protection remain undefined. Also, several studies have investigated NK cell
321 memory upon BCG vaccination but resulted in different conclusions. Kawahara, Hasegawa,

and Takaku 2016 showed that purified splenic NK cells from BCG vaccinated mice do not produce more IFNγ or enhance macrophage phagocytosis in the presence of BCG *in vitro*. However, Venkatasubramanian et al. 2017 suggested that a subset of $CD27^+$ $KLRG1^+$ NK cells expand following BCG inoculation and confer protection against *M. tuberculosis* infection by reducing the CFU numbers in the lungs at 30 days post-infection. Finally, it has been shown that BCG immunization may induce antigen-independent memory-like NK cells that can protect mice to heterologous challenge with *Candida albicans* (Kleinnijenhuis et al. 2014). Altogether, these studies, along with our work, indicate that NK cell memory could be a general feature of NK cells to all bacteria, and could have important functions during infection.

It remains undefined how NK cells sense and respond to bacteria. Activating receptors are engaged upon sensing of cells infected with intracellular bacteria (Mody et al. 2019), however, NK cell interactions with extracellular bacteria are poorly explored. One study on human NK cells reported an engagement between the inhibitory receptor Siglec-7 and the β-protein on the surface of group B Streptococcus (Fong et al., 2018). However, neither Siglec-7, nor a homologue, is expressed in mice, and thus NK cell binding-interactions with extracellular bacteria are undefined. In our model, we have shown *in vitro* that purified NK cells can be directly activated upon incubation with only IL-15+IL-18 and *S. pneumoniae*. Therefore, our data strongly suggest that NK cells directly interact with bacteria thereby inducing cell responses. Such interaction could occur through an unknown surface receptor recognizing some component of the pneumococcal capsule or membrane.

Previous studies have shown that memory or memory-like NK cells to viruses and cytokines display increased IFNγ secretion upon re-stimulation (Sun, Beilke, and Lanier 2009; Cooper et al., 2009). Furthermore, endotoxemia-induced memory-like NK cells were also described to produce more IFNγ following *in vivo* secondary LPS injection (Rasid et al., 2019). Altogether, it suggests that IFNγ production is the main effector function of memory NK cells

in these models. However, in our model, although we detected an increase of IFNγ$^+$ NK cells *in vitro*, the protective effect of memory NK cells was not dependent on IFNγ. In fact, the absence of IFNγ signaling in recipient mice did not affect bacterial dissemination and neutrophils recruitment at early timepoints. Furthermore, we showed less IFNγ$^+$ NK cells in the lungs of infected mice receiving memory NK cells. Interestingly, NK cells display a slight remodeling of chromatin at an IFNγ enhancer suggesting that at the epigenetic level, memory NK cells are ready to produce more IFNγ upon the proper stimulus, such as that provided *in vitro*. Surprisingly, we find no evidence that IFNγ is playing a role in our mouse model and the reduced production of cytokines in the lungs of protected mice could be the consequence of lower number of bacteria in those animals.

The function of NK cells in the recruitment of inflammatory cells is well defined, so is their role in cytotoxicity of infected cells. Indeed, the release of cytotoxic molecules into the immune synapse to induce apoptosis of infected cells is well described (Chowdhury and Lieberman 2008; Voskoboinik, Whisstock, and Trapani 2015). Granules secreted by NK cells contain the pore-forming protein Perforin which damages the target cell membrane allowing Granzymes to pass, resulting in the activation of the caspase pathway and reactive oxygen species (ROS) production. Interestingly, the release of Granulysin and Granzyme B into the cytosol of infected cells targets intracellular bacteria (Walch et al. 2014). However, the importance of NK cell cytotoxicity in the context of extracellular bacterial infections is not well understood. A few intriguing *in vitro* studies report direct receptor-mediated recognition and killing of extracellular bacteria such as *Mycobacterium tuberculosis*, *Burkholderia cenocepacia* or *Pseudomonas aeruginosa* by NK cell degranulation (Lu et al., 2014; Li et al., 2019; Feehan et al., 2022). Recognition of bacteria by NK cells has been suggested to be receptor mediated as soluble NKp44 binding to extracellular *Mycobacterium tuberculosis* was shown *in vitro* (Esin et al. 2008). However, neither bacterial recognition nor direct killing has been

372 demonstrated during an *in vivo* infection, and the mechanisms at play are unknown. In our
373 model of extracellular bacterial infection *in vivo*, we have shown that memory NK cells lead to
374 more Granzyme B production in the lungs of protected mice, suggesting this effector protein
375 could contribute to host protection against *S. pneumoniae*.

376 NK cell-based therapies are the basis of a new generation of innovative immunotherapy
377 for cancer, which yields encouraging results in clinical trials (Shimasaki, Jain, and Campana
378 2020). It is based on activation of NK cells *ex vivo* for heightened activity against tumor cells.
379 Our work, along with the extensive knowledge on NK cell memory to viruses, could suggest
380 similar *ex vivo* activation strategies against infections. Gaining a greater understanding of the
381 mechanisms at play as well as the memory features will be paramount.

382

383 **Materials and Methods**

384

385 **Animal model.** All protocols for animal experiments were reviewed and approved by the
386 CETEA (Comité d'Ethique pour l'Expérimentation Animale- Ethics Committee for Animal
387 Experimentation) of the Institut Pasteur under approval number dap170005 and were performed
388 in accordance with national laws and institutional guidelines for animal care and use.
389 Experiments were conducted using C57BL/6J females of 7 to 12 weeks of age. CD45.2 mice
390 were purchased from Janvier Labs (France). CD45.1, *Ifngr*1$^{-/-}$ (JAX stock #003288) and *Prf*1$^{-/-}$
391 (JAX stock #002407) mice were maintained in house at the Institut Pasteur animal facility.

392

393 **Bacterial inocula.** All experiments that include infection with *Streptococcus pneumoniae* were
394 conducted with the luminescent serotype 4 TIGR4 strain (Ci49) (containing pAUL-A Tn*4001*
395 *luxABCDE* Km', (Saleh et al. 2014)), and obtained from Thomas Kohler, Universität
396 Greifswald. Experimental starters were prepared from frozen master stocks plated on 5%

Columbia blood agar plates (Biomerieux ref no.43041) and grown overnight at 37°C with 5% CO_2 prior to outgrowth in Todd-Hewitt (BD) broth supplemented with 50mM HEPES (TH+H) and kanamycin (50 µg/ml), as previously described in (Connor et al. 2021). Inoculum were prepared from frozen experimental starters grown to midlog phase in TH+H broth supplement with kanamycin (50 µg/ml) at 37°C with 5% CO_2 in unclosed falcon tubes. Bacteria were pelleted at 1500xg for 10 min at room temperature, washed three times in DPBS and resuspended in DPBS at the desired cfu/ml. Bacterial cfu enumeration was determined by serial dilution plating on 5% Columbia blood agar plates.

Listeria monocytogenes EGD strain were grown overnight in brain heart infusion (BHI) liquid broth with shaking at 37°C. Overnight culture were then subcultured 1/10 into fresh BHI and grown to an OD600 of 1. Bacteria were washed three times and subsequently resuspended in DPB. Experimental starters were then frozen at -80. For mouse infections, experimental starters were thawed on ice and diluted in fresh DPBS at the desired cfu/ml.

For bacteria killed with paraformaldehyde (PFA), the concentrated bacteria, prior to dilution, were incubated in 4% PFA for 30 minutes at room temperature, washed in DPBS and diluted to the desired cfu/ml.

Mouse infection. Animals were anaesthetized with a ketamine and xylazine cocktail (intra-muscular injection) prior to infection. Mice were infected with *Streptococcus pneumoniae* by intranasal instillation of 20µl containing $5x10^5$ (sub-lethal dose), $5x10^6$ (survival study) or $1x10^7$ cfu (lethal dose). Control mice received intranasal injection of 20µl of DPBS. For *Listeria monocytogenes* infection, mice were injected with 100µl of $1x10^6$ cfu by retro-orbital injection. Animals were monitored daily for the first 5 days and then weekly for the duration of the experiment. Mouse sickness score from (Stark et al. 2018) was used to assess progression of mice throughout *S. pneumoniae* infection, representing the following scores: 0- Healthy; 1-

transiently reduced response/slightly ruffled coat/transient ocular discharge/up to 10% weight loss; 2 and 3- (2-up to 2 signs, 3- up to 3 signs) clear piloerection/intermittent hunched posture/persistent oculo-nasal discharge/persistently reduced response/intermittent abnormal breathing/up to 15% weight loss; 4-death. Animals were euthanized by CO_2 asphyxiation at ≥ 20% loss of initial weight or at persistent clinical score 3.

Sampling. The nasal lavage was obtained by blocking the oropharynx to avoid leakage into the oral cavity and lower airway, and nares were flushed two times with 500µl DPBS. Bronchio-alveolar fluid (BALF) was collected by inserting catheter (18GA 1.16IN, 1.3x30 mm) into the trachea and washing the lungs with 2ml of DPBS. Blood was collected by cardiac puncture at left ventricle with 20G needle and immediately mixed with 100mM EDTA to prevent coagulation. Spleens were disrupted by mechanical dissociation using curved needles to obtain splenocytes suspension in DPBS supplemented with 0,5% FCS+0,4% EDTA. Lungs were mechanically dissociated with gentleMACS Dissociator (Miltenyi Biotec) in cTubes containing lung dissociation kit reagents (DNAse and collagenase ref no.130-095-927, Miltenyi Biotec). Lungs, BALF, nasal lavage, blood, spleen homogenates were plated in serial dilutions on 5% Columbia blood agar plates supplemented with gentamycin (5µg/ml) to determine bacterial counts.

NK cell purification and transfer. Splenocytes were passed successively through 100µm, 70µm and 30µm strainers (Miltenyi Biotec) in DPBS (+0,5% FCS+0,4% EDTA) and counted for downstream applications. NK cells were first enriched from splenocytes suspensions using negative enrichment kit (Invitrogen, ref no.8804-6828) according to manufacturer's protocol but combined with separation over magnetic columns (LS columns, Miltenyi Biotec). NK cells were then re-purified by negative selection using purification kit and magnetic columns

447 according to manufacturer's instructions to reach purities of approximately 98% (Miltenyi
448 Biotec, MS columns and isolation kit ref no.130-115-818). Purified NK cells were transferred
449 intravenously by retro-orbital injections into recipient mice (0,2-1.10^6 cells/mouse) in 100µl of
450 DPBS or cultured for *in vitro* experiments.
451
452 **NK cell culture.** Purified NK cells were cultured at 1.10^6 cells/ml in 200µl RPMI 1640 (Gibco)
453 supplemented with 10% FCS and 1 U/mL Penicillin-Streptomycin (10 000 U/mL, Gibco) in 96
454 well round-bottom plates. Cells were either left unstimulated or activated with
455 paraformaldehyde inactivated bacteria at MOI 20 (*S. pneumoniae*, L. *monocytogenes* or *S.*
456 *agalactiae)* and/or with various cytokine cocktails composed of IL-15 (2 ng/ml), IL-18 (1,5
457 ng/ml) and IL-12 (1,25 ng/ml) (Miltenyi Biotec). After 20 hours of culture at 37°C, 1X
458 Brefeldin-A (BFA solution 1000X, ref no.420601, BioLegend) was added into each well to
459 block secretion of IFNγ for 4 hours. After incubation at 37°C, cells were collected for
460 intracellular cytokine and cytotoxic proteins by flow cytometry.
461
462 **Cell preparation for cytometry staining**. Following mechanical dissociation, lung and spleen
463 homogenates were passed through 100µm strainers in DPBS supplemented with 0,5%
464 FCS+0,4% EDTA, lysed in 1X red blood cell lysis buffer for 3 minutes (ref no. 420301,
465 BioLegend), and passed successively through 70µm and 30µm strainers (Miltenyi Biotec).
466 Single cell suspensions from BALF, lung and spleen were counted and prepared for surface
467 staining in 96 well plates. Prior to IFNγ staining, single cell suspensions are incubated with 1X
468 Brefeldin-A for 4 hours at 37°C to block secretion of cytokines (ref no.420601, BioLegend).
469 For all, cells were first stained with anti-mouse CD16/CD32 to block unspecific binding and a
470 cocktail of surface labeling antibodies for 40 minutes in DPBS (+0,5% FCS+0,4% EDTA).
471 Next, cells were stained for viability using fixable viability dye (eFluor780, ref no.65-0865-14,

Invitrogen) for 5 minutes at 4°C and then fixed using commercial fixation buffer for 3 minutes (ref no. 420801, BioLegend). For intracellular staining of Granzyme B and Perforin, cells were permeabilized with a Fixation/Permeabilization commercial kit for 30 minutes (Concentrate and Diluent, ref no. 00-5123-43, Invitrogen). After permeabilization and wash, cells were stained with respective antibodies in DPBS (+0,5% FCS+0,4% EDTA) overnight at 4°C. For intracellular staining of IFNγ, cells were permeabilized and stained in buffer from commercial kit (Inside Stain Kit, ref no. 130-090-477, Miltenyi Biotec) for 40 minutes at 4°C. After a final wash suspended in DPBS, sample acquisitions were performed on MACSQuant (Miltenyi Biotec) and LSRFortessa (BD Biosciences) flow-cytometers and analysis were done using FlowJo Software (TreeStar).

ELISA. Following mechanical dissociation, lung homogenates are centrifuged at 400xg for 7 minutes at 4°C. Supernatants are collected and frozen at -20°C for cytokine assays performed by ELISA according to manufacturer's instructions (DuoSet, R&D Systems).

ChIP-qPCR assays. Around 4.10^6-6.10^6 NK cells were fixed in 1% formaldehyde (8 min, room temperature), and the reaction was stopped by the addition of glycine at the final concentration of 0,125 M. After two washes in PBS, cells were resuspended in 0.25% Triton X-100, 10 mM Tris-HCl (pH 8), 10 mM EDTA, 0.5 mM EGTA and proteases inhibitors; the soluble fraction was eliminated by centrifugation; and chromatin was extracted with 250 mM NaCl, 50 mM Tris-HCl (pH 8), 1 mM EDTA, 0.5 mM EGTA and proteases inhibitors cocktail for 30 min on ice. Chromatin was resuspended in 1% SDS, 10 mM Tris-HCl (pH 8), 1 mM EDTA, 0.5 mM EGTA and proteases inhibitors cocktail; and sonicated during 10 cycles using Diagenode Bioruptor Pico (30 sec on 30 sec off). DNA fragment size (<1 kb) was verified by agarose gel electrophoresis. ChIP was performed using H3K4me1 antibody and nonimmune

IgG (negative control antibody), 10 µg chromatin per condition was used. Chromatin was diluted 10 times in 0.6% Triton X-100, 0.06% sodium deoxycholate (NaDOC), 150 mM NaCl, 12 mM Tris-HCl, 1 mM EDTA, 0.5 mM EGTA and proteases inhibitors cocktail. For 6 hours, the different antibodies were previously incubated at 4°C with protein G-coated magnetic beads (DiaMag, Diagenode), protease inhibitor cocktail and 0.1% BSA. Chromatin was incubated overnight at 4°C with each antibody/protein G-coated magnetic beads. Immunocomplexes were washed with 1 x buffer 1 (1% Triton X-100, 0.1% NaDOC, 150 mM NaCl, 10 mM Tris-HCl (pH 8)), 1 x buffer 2 (0.5% NP-40, 0.5% Triton X-100, 0.5 NaDOC, 150 mM NaCl, 10 mM Tris-HCl (pH 8)), 1 x buffer 3 (0.7% Triton X-100, 0.1% NaDOC, 250 mM NaCl, 10 mM Tris-HCl (pH 8)) 1 x buffer 4 (0.5% NP-40, 0.5% NaDOC, 250 mM LiCl, 20 mM Tris-HCl (pH 8), 1 mM EDTA) and 1 x buffer 5 (0,1% NP-40, 150 mM NaCl, 20 mM Tris-HCl (pH 8), 1 mM EDTA). Beads were eluted in water containing 10% Chelex and reverse cross-linked by boiling for 10 min, incubating with RNase for 10 min at room temperature, then with proteinase K for 20 min at 55°C and reboiling for 10 min. DNA fragment were purified by Phenol Chloroform extraction. Amplifications (40 cycles) were performed using quantitative real-time PCR using iTaq™ Universal Syber Green Supermix (BIORAD) on a CFX384 Touch Real-Time PCR system (BIORAD). qPCR efficiency (E) was determined for the ChIP primers with a dilution series of genomic mouse DNA. The threshold cycles (Ct values) were recorded from the exponential phase of the qPCR for IP and input DNA for each primer pair. The relative amount of immunoprecipitated DNA was compared to input DNA for the control regions (% of recovery) using the following formula:

% recovery = E^((Ct(1% input) - Log_2(input dilution)) – Ct (IP)) x 100%

<u>Primer sequences</u>

-22kb enhancer of the IFNγ locus

5'CCAGGACAGAGGTGTTAAGCCA3'

5'GCAACTTCTTTCTTCTCAGGGTG3'

-55kb enhancer of the IFNγ locus

5'GGCTTCCTGTCATTGTTTCCA3'

5'CAGAGCCATGGGATGACTGA3'

-34kb enhancer of Granzyme B locus

5'CCCTCCCCTCTAATCACACA3'

5'ACGGTGTTGAGGGAGTTTCA3'

Intergenic Region (IG)

5'CCACACCTCTTCCTTCTGGA3'

5'ATTTGTGTCAGAGCCCAAGC3'

Quantification and statistical analysis. Statistical significance was tested using Prism 9 Software (GraphPad). Mann Whitney test was used for single comparisons, Kruskal-Wallis test for 3 groups- comparisons, 2way ANOVA for multiple comparisons and Log-rank (Mantel-Cox) test for survival curves.

Acknowledgements

We thank P. Bousso (Institut Pasteur) and M. Lecuit (Institut Pasteur) for their generous gifts of *Ifngr*1$^{-/-}$ and *Prf*1$^{-/-}$ mice. We are thankful to M. Ingersoll for her precious advice throughout

the project and corrections of the manuscript. We would like to thank E. Gomez Perdiguero for her help with flow cytometry analysis. We thank P.H. Commere and S. Megharba (Cytometry and Biomarkers UTechS, Institut Pasteur) for their help with flow cytometry acquisition. T.M.N.C is supported by the Fondation pour la Recherche Médicale, grants no. PMJ201810007628 (Prix MARIANE JOSSO) and no. FDT202106012790 (Fin de thèse), a donation from Mécénat Crédit Agricole Ile-de-France, and Institut Pasteur. J.T is supported by the Fondation ARC, grant no. ARCPOST-DOC2021070004074. M.A.H. is supported by the Institut Pasteur, the Agence Nationale de la Recherche (ANR-17-CE12-0007), the Fondation pour la Recherche Médicale (EQU202003010152), the Fondation iXCore-iXLife, and is a member of the Laboratoire d'Excellence "Integrative Biology of Emerging Infectious Diseases" Agence Nationale de la Recherche (ANR): ANR-10-LABX- 62-EIBID).

Author contributions

T.C. coordinated the study. M.A.H. conceived and designed the study. T.C., J.T. and C.C performed experiments and analyzed data. T.C. and M.A.H. conceived and wrote the manuscript. O.R. and M.A.H. supervised the work.

References

Azzi, Tarik, Anita Murer, Seigo Ueda, Karl-Johan Malmberg, Georg Staubli, Claudine Gysin, Christoph Berger, Obinna Chijioke, and David Nadal. 2014. "Role for Early-Differentiated Natural Killer Cells in Infectious Mononucleosis." *Blood* 124 (16): 2533–43. https://doi.org/10.1182/blood-2014-01.

Baranek, Thomas, Eric Morello, Alexandre Valayer, Rose France Aimar, Déborah Bréa, Clemence Henry, Anne Gaelle Besnard, et al. 2017. "FHL2 Regulates Natural Killer Cell Development and Activation during Streptococcus Pneumoniae Infection." *Frontiers in Immunology* 8 (123). https://doi.org/10.3389/fimmu.2017.00123.

575 Bogaert, D., R. de Groot, and P. W.M. Hermans. 2004. "Streptococcus Pneumoniae
576 Colonisation: The Key to Pneumococcal Disease." *Lancet Infectious Diseases*.
577 https://doi.org/10.1016/S1473-3099(04)00938-7.
578 Cerwenka, Adelheid, and Lewis L. Lanier. 2016. "Natural Killer Cell Memory in Infection,
579 Inflammation and Cancer." *Nature Reviews Immunology*. Nature Publishing Group.
580 https://doi.org/10.1038/nri.2015.9.
581 Chowdhury, Dipanjan, and Judy Lieberman. 2008. "Death by a Thousand Cuts: Granzyme
582 Pathways of Programmed Cell Death." *Annual Review of Immunology*.
583 https://doi.org/10.1146/annurev.immunol.26.021607.090404.
584 Christaki, Eirini, Evdoxia Diza, Evangelos J. Giamarellos-Bourboulis, Nikoletta
585 Papadopoulou, Aikaterini Pistiki, Dionysia Irini Droggiti, Marianna Georgitsi, et al. 2015.
586 "NK and NKT Cell Depletion Alters the Outcome of Experimental Pneumococcal
587 Pneumonia: Relationship with Regulation of Interferon- γ Production." *Journal of*
588 *Immunology Research* 2015. https://doi.org/10.1155/2015/532717.
589 Clark, Sarah E., Rebecca L. Schmidt, Elizabeth R. Aguilera, and Laurel L. Lenz. 2020. "IL-10-
590 Producing NK Cells Exacerbate Sublethal Streptococcus Pneumoniae Infection in the
591 Lung." *Translational Research* 226 (December): 70–82.
592 https://doi.org/10.1016/j.trsl.2020.07.001.
593 Connor, Michael G., Tiphaine M.N. Camarasa, Emma Patey, Orhan Rasid, Laura Barrio,
594 Caroline M. Weight, Daniel P. Miller, et al. 2021. "The Histone Demethylase KDM6B
595 Fine-Tunes the Host Response to Streptococcus Pneumoniae." *Nature Microbiology* 6 (2):
596 257–69. https://doi.org/10.1038/s41564-020-00805-8.
597 Cooper, Megan A, Julie M Elliott, Peter A Keyel, Liping Yang, Javier A Carrero, and Wayne
598 M Yokoyama. 2009. "Cytokine-Induced Memory-like Natural Killer Cells." *PNAS* 106
599 (6): 1915–19. www.pnas.org/cgi/content/full/.
600 Divangahi, Maziar, Peter Aaby, Shabaana Abdul Khader, Luis B. Barreiro, Siroon Bekkering,
601 Triantafyllos Chavakis, Reinout van Crevel, et al. 2021. "Trained Immunity, Tolerance,
602 Priming and Differentiation: Distinct Immunological Processes." *Nature Immunology*.
603 Nature Research. https://doi.org/10.1038/s41590-020-00845-6.
604 Dornand, Jacques, Virginie Lafont, Jane Oliaro, Annie Terraza, Elsa Castaneda-Roldan, and
605 Jean Pierre Liautard. 2004. "Impairment of Intramacrophagic Brucella Suis Multiplication
606 by Human Natural Killer Cells Through A Contact-Dependent Mechanism." *Infection and*
607 *Immunity* 72 (4): 2303–11. https://doi.org/10.1128/IAI.72.4.2303-2311.2004.
608 Elhaik-Goldman, Shirin, Daniel Kafka, Rami Yossef, Uzi Hadad, Moshe Elkabets, Alexandra
609 Vallon-Eberhard, Luai Hulihel, et al. 2011. "The Natural Cytotoxicity Receptor 1
610 Contribution to Early Clearance of Streptococcus Pneumoniae and to Natural Killer-
611 Macrophage Cross Talk." *PLoS ONE* 6 (8). https://doi.org/10.1371/journal.pone.0023472.
612 Esin, Semih, Giovanna Batoni, Claudio Counoupas, Annarita Stringaro, Franca Lisa
613 Brancatisano, Marisa Colone, Giuseppantonio Maisetta, Walter Florio, Giuseppe Arancia,
614 and Mario Campa. 2008. "Direct Binding of Human NK Cell Natural Cytotoxicity
615 Receptor NKp44 to the Surfaces of Mycobacteria and Other Bacteria." *Infection and*
616 *Immunity* 76 (4): 1719–27. https://doi.org/10.1128/IAI.00870-07.
617 Feehan, David D., Khusraw Jamil, Maria J. Polyak, Henry Ogbomo, Mark Hasell, Shu Shun
618 Li, Richard F. Xiang, et al. 2022. "Natural Killer Cells Kill Extracellular Pseudomonas
619 Aeruginosa Using Contact-Dependent Release of Granzymes B and H." *PLoS Pathogens*
620 18 (2). https://doi.org/10.1371/journal.ppat.1010325.
621 Feng, Carl G., Mallika Kaviratne, Antonio Gigliotti Rothfuchs, Allen Cheever, Sara Hieny,
622 Howard A. Young, Thomas A. Wynn, and Alan Sher. 2006. "NK Cell-Derived IFN-γ
623 Differentially Regulates Innate Resistance and Neutrophil Response in T Cell-Deficient

624 Hosts Infected with Mycobacterium Tuberculosis." *The Journal of Immunology* 177 (10):
625 7086–93. https://doi.org/10.4049/jimmunol.177.10.7086.
626 Fernandes, Dancella M, Rita Benson, and Cynthia L Baldwin. 1995. "Lack of a Role for Natural
627 Killer Cells in Early Control of Brucella Abortus 2308 Infections in Mice." *Infection and*
628 *Immunity* 63 (10): 4029–33.
629 Fong, Jerry J., Chih Ming Tsai, Sudeshna Saha, Victor Nizet, Ajit Varki, and Jack D. Buif.
630 2018. "Siglec-7 Engagement by GBS β-Protein Suppresses Pyroptotic Cell Death of
631 Natural Killer Cells." *Proceedings of the National Academy of Sciences of the United*
632 *States of America* 115 (41): 10410–15. https://doi.org/10.1073/pnas.1804108115.
633 Geary, Clair D., and Joseph C. Sun. 2017. "Memory Responses of Natural Killer Cells."
634 *Seminars in Immunology*. Academic Press. https://doi.org/10.1016/j.smim.2017.08.012.
635 Gillespie, S H, and I Balakrishnan. 2000. "Pathogenesis of Pneumococcal Infection." *J. Med.*
636 *Microbiol* 49: 1057–67. www.microbiologyresearch.org.
637 Goldmann, Oliver, Gursharan S Chhatwal, and Eva Medina. 2005. "Contribution of Natural
638 Killer Cells to the Pathogenesis of Septic Shock Induced by Streptococcus Pyogenes in
639 Mice." *The Journal of Infectious Diseases* 191: 1280–86.
640 https://academic.oup.com/jid/article/191/8/1280/859945.
641 Gonzales, Christine M., Courtney B. Williams, Veronica E. Calderon, Matthew B. Huante,
642 Scott T. Moen, Vsevolod L. Popov, Wallace B. Baze, Johnny W. Peterson, and Janice J.
643 Endsley. 2012. "Antibacterial Role for Natural Killer Cells in Host Defense to Bacillus
644 Anthracis." *Infection and Immunity* 80 (1): 234–42. https://doi.org/10.1128/IAI.05439-11.
645 Habib, Samar, Abdeljabar el Andaloussi, Ahmed Hisham, and Nahed Ismail. 2016. "NK Cell-
646 Mediated Regulation of Protective Memory Responses against Intracellular Ehrlichial
647 Pathogens." *PLoS ONE* 11 (4). https://doi.org/10.1371/journal.pone.0153223.
648 Hamon, Melanie A., and Jessica Quintin. 2016. "Innate Immune Memory in Mammals."
649 *Seminars in Immunology* 28 (4): 351–58. https://doi.org/10.1016/j.smim.2016.05.003.
650 Ivin, Masa, Amy Dumigan, Filipe N. de Vasconcelos, Florian Ebner, Martina Borroni, Anoop
651 Kavirayani, Kornelia N. Przybyszewska, et al. 2017. "Natural Killer Cell-Intrinsic Type I
652 IFN Signaling Controls Klebsiella Pneumoniae Growth during Lung Infection." *PLoS*
653 *Pathogens* 13 (11). https://doi.org/10.1371/journal.ppat.1006696.
654 Junqueira-Kipnis, Ana Paula, Andre Kipnis, Amanda Jamieson, Mercedes Gonzalez Juarrero,
655 Andreas Diefenbach, David H. Raulet, Joanne Turner, and Ian M. Orme. 2003. " NK Cells
656 Respond to Pulmonary Infection with Mycobacterium Tuberculosis , but Play a Minimal
657 Role in Protection ." *The Journal of Immunology* 171 (11): 6039–45.
658 https://doi.org/10.4049/jimmunol.171.11.6039.
659 Kadioglu, Aras, Jeffrey N. Weiser, James C. Paton, and Peter W. Andrew. 2008. "The Role of
660 Streptococcus Pneumoniae Virulence Factors in Host Respiratory Colonization and
661 Disease." *Nature Reviews Microbiology*. https://doi.org/10.1038/nrmicro1871.
662 Kawahara, Mamoru, Nozomi Hasegawa, and Hiroshi Takaku. 2016. "Murine Splenic Natural
663 Killer Cells Do Not Develop Immunological Memory after Re-Encounter with
664 Mycobacterium Bovis Bcg." *PLoS ONE* 11 (3).
665 https://doi.org/10.1371/journal.pone.0152051.
666 Kerr, Alison R., Lea Ann S. Kirkham, Aras Kadioglu, Peter W. Andrew, Paul Garside, Hal
667 Thompson, and Tim J. Mitchell. 2005. "Identification of a Detrimental Role for NK Cells
668 in Pneumococcal Pneumonia and Sepsis in Immunocompromised Hosts." *Microbes and*
669 *Infection* 7 (5–6): 845–52. https://doi.org/10.1016/j.micinf.2005.02.011.
670 Kleinnijenhuis, Johanneke, Jessica Quintin, Frank Preijers, Leo A.B. Joosten, Cor Jacobs,
671 Ramnik J. Xavier, Jos W.M. van der Meer, Reinout van Crevel, and Mihai G. Netea. 2014.
672 "BCG-Induced Trained Immunity in NK Cells: Role for Non-Specific Protection to

673 Infection." *Clinical Immunology* 155 (2): 213–19.
674 https://doi.org/10.1016/j.clim.2014.10.005.
675 Lai, Hsin-Chih, Chih-Jung Chang, Chuan-Sheng Lin, Tsung-Ru Wu, Ya-Jing Hsu, Ting-Shu
676 Wu, Jang-Jih Lu, et al. 2018. "NK Cell–Derived IFN-γ Protects against Nontuberculous
677 Mycobacterial Lung Infection." *The Journal of Immunology* 201 (5): 1478–90.
678 https://doi.org/10.4049/jimmunol.1800123.
679 Lau, Colleen M, Gabriela M Wiedmann, and Joseph C Sun. 2022. "Epigenetic Regulation of
680 Natural Killer Cell Memory." *Immunological Reviews* 305: 90–110.
681 Li, Shu Shun, Marwah Saleh, Richard F. Xiang, Henry Ogbomo, Danuta Stack, Shaunna H.
682 Huston, and Christopher H. Mody. 2019. "Natural Killer Cells Kill Burkholderia Cepacia
683 Complex via a Contact-Dependent and Cytolytic Mechanism." *International Immunology*
684 31 (6): 385–96. https://doi.org/10.1093/intimm/dxz016.
685 Littwitz-Salomon, Elisabeth, Thanh Nguyen, Simone Schimmer, and Ulf Dittmer. 2018.
686 "Friend Retrovirus Infection Induces the Development of Memory-like Natural Killer
687 Cells 11 Medical and Health Sciences 1107 Immunology." *Retrovirology* 15 (1).
688 https://doi.org/10.1186/s12977-018-0450-1.
689 Lopez-Vergès, Sandra, Jeffrey M. Milush, Brian S. Schwartz, Marcelo J. Pando, Jessica
690 Jarjoura, Vanessa A. York, Jeffrey P. Houchins, et al. 2011. "Expansion of a Unique CD57
691 +NKG2C Hi Natural Killer Cell Subset during Acute Human Cytomegalovirus Infection."
692 *Proceedings of the National Academy of Sciences of the United States of America* 108
693 (36): 14725–32. https://doi.org/10.1073/pnas.1110900108.
694 Lu, Chia-Chen, Ting-Shu Wu, Ya-Jing Hsu, Chih-Jung Chang, Chuan-Sheng Lin, Ju-Hsin
695 Chia, Tsu-Lan Wu, et al. 2014. "NK Cells Kill Mycobacteria Directly by Releasing
696 Perforin and Granulysin." *Journal of Leukocyte Biology* 96 (6): 1119–29.
697 https://doi.org/10.1189/jlb.4a0713-363rr.
698 Mody, Christopher H., Henry Ogbomo, Richard F. Xiang, Stephen K. Kyei, David Feehan,
699 Anowara Islam, and Shu Shun Li. 2019. "Microbial Killing by NK Cells." *Journal of*
700 *Leukocyte Biology*. John Wiley and Sons Inc. https://doi.org/10.1002/JLB.MR0718-298R.
701 O'Sullivan, Timothy E., Joseph C. Sun, and Lewis L. Lanier. 2015. "Natural Killer Cell
702 Memory." *Immunity*. Cell Press. https://doi.org/10.1016/j.immuni.2015.09.013.
703 Quintin, Jessica, Shih Chin Cheng, Jos W.M. van der Meer, and Mihai G. Netea. 2014. "Innate
704 Immune Memory: Towards a Better Understanding of Host Defense Mechanisms."
705 *Current Opinion in Immunology*. Elsevier Ltd. https://doi.org/10.1016/j.coi.2014.02.006.
706 Rasid, Orhan, Christine Chevalier, Tiphaine Marie Noelle Camarasa, Catherine Fitting, Jean
707 Marc Cavaillon, and Melanie Anne Hamon. 2019. "H3K4me1 Supports Memory-like NK
708 Cells Induced by Systemic Inflammation." *Cell Reports* 29 (12): 3933-3945.e3.
709 https://doi.org/10.1016/j.celrep.2019.11.043.
710 Saeed, Sadia, Jessica Quintin, Hindrik H D Kerstens, Nagesha A Rao, Ali Aghajanirefah,
711 Filomena Matarese, Shih-Chin Cheng, et al. 2014. "Epigenetic Programming of
712 Monocyte-to-Macrophage Differentiation and Trained Innate Immunity." *Science* 345
713 (6204): 1251086–10. www.ihec-epigenomes.
714 Saleh, Malek, Mohammed R. Abdullah, Christian Schulz, Thomas Kohler, Thomas Pribyl, Inga
715 Jensch, and Sven Hammerschmidt. 2014. "Following in Real Time the Impact of
716 Pneumococcal Virulence Factors in an Acute Mouse Pneumonia Model Using
717 Bioluminescent Bacteria." *Journal of Visualized Experiments*, no. 84 (February).
718 https://doi.org/10.3791/51174.
719 Shimasaki, Noriko, Amit Jain, and Dario Campana. 2020. "NK Cells for Cancer
720 Immunotherapy." *Nature Reviews Drug Discovery*. Nature Research.
721 https://doi.org/10.1038/s41573-019-0052-1.

Spörri, Roman, Nicole Joller, Urs Albers, Hubert Hilbi, and Annette Oxenius. 2006. "MyD88-Dependent IFN-γ Production by NK Cells Is Key for Control of Legionella Pneumophila Infection." *The Journal of Immunology* 176 (10): 6162–71. https://doi.org/10.4049/jimmunol.176.10.6162.

Stark, Anne-Katrien, Anne-Katrien Stark, Edward Banham-Hall, and Klaus Okkenhaug. 2018. "Acute Streptococcus Pneumoniae Lung Infection: Mouse Model and Characterisation of the Immune Response." *Protocol Exchange*, September. https://doi.org/10.1038/protex.2018.114.

Sun, Joseph C., Joshua N. Beilke, and Lewis L. Lanier. 2009. "Adaptive Immune Features of Natural Killer Cells." *Nature* 457 (7229): 557–61. https://doi.org/10.1038/nature07665.

Theresine, Maud, Neha D. Patil, and Jacques Zimmer. 2020. "Airway Natural Killer Cells and Bacteria in Health and Disease." *Frontiers in Immunology*. Frontiers Media S.A. https://doi.org/10.3389/fimmu.2020.585048.

Venkatasubramanian, S., S. Cheekatla, P. Paidipally, D. Tripathi, E. Welch, A. R. Tvinnereim, R. Nurieva, and R. Vankayalapati. 2017. "IL-21-Dependent Expansion of Memory-like NK Cells Enhances Protective Immune Responses against Mycobacterium Tuberculosis." *Mucosal Immunology* 10 (4): 1031–42. https://doi.org/10.1038/mi.2016.105.

Voskoboinik, Ilia, James C. Whisstock, and Joseph A. Trapani. 2015. "Perforin and Granzymes: Function, Dysfunction and Human Pathology." *Nature Reviews Immunology*. Nature Publishing Group. https://doi.org/10.1038/nri3839.

Walch, Michael, Farokh Dotiwala, Sachin Mulik, Jerome Thiery, Tomas Kirchhausen, Carol Clayberger, Alan M. Krensky, Denis Martinvalet, and Judy Lieberman. 2014. "Cytotoxic Cells Kill Intracellular Bacteria through Granulysin-Mediated Delivery of Granzymes." *Cell* 157 (6): 1309–23. https://doi.org/10.1016/j.cell.2014.03.062.

Wang, Dongfang, Xiuling Gu, Xiaoman Liu, Songtao Wei, Bin Wang, and Min Fang. 2018. "NK Cells Inhibit Anti-Mycobacterium Bovis BCG T Cell Responses and Aggravate Pulmonary Inflammation in a Direct Lung Infection Mouse Model." *Cellular Microbiology* 20 (7). https://doi.org/10.1111/cmi.12833.

Weiser, Jeffrey N., Daniela M. Ferreira, and James C. Paton. 2018. "Streptococcus Pneumoniae: Transmission, Colonization and Invasion." *Nature Reviews Microbiology*. Nature Publishing Group. https://doi.org/10.1038/s41579-018-0001-8.

Wijaya, Ratna S., Scott A. Read, Naomi R. Truong, Shuanglin Han, Dishen Chen, Haleh Shahidipour, Nicole L. Fewings, et al. 2021. "HBV Vaccination and HBV Infection Induces HBV-Specific Natural Killer Cell Memory." *Gut* 70 (2): 357–69. https://doi.org/10.1136/gutjnl-2019-319252.

Legends

Figure 1: NK cells acquire intrinsic memory features 21 days after *in vivo* infection.

(A) Experimental scheme. C57BL/6 mice were intranasally injected with either PBS (black symbols) or sub-lethal dose of *S. pneumoniae* (SPN, red symbols, 5.10^5 CFU) for two consecutive days. After 21 days, NK cells were highly purified from spleens of D21PBS or

765 D21SPN mice (98% of purity) and stimulated *in vitro* with cytokines (IL-15 at 2 ng/ml, IL-18
766 at 1,5 ng/ml, IL-12 at 1,25 ng/ml) and formaldehyde inactivated *S. pneumoniae* (SPN, MOI 20)
767 for 24 hours.
768 **(B)** Intensity of IFNγ expression in NK cells (MFI, **left panel**), percentage of IFNγ^+ NK cells
769 (**middle panel**), representative overlay histogram upon IL-15+IL-18+SPN stimulation (**right**
770 **panel**, gray represents isotype control). Box plots where each dot represents a pool of mice
771 from one experiment (black dots for D21PBS NKs, red dots for D21SPN NKs), lines are
772 median, error bars show min to max. Data are representative of at least three experiments with
773 $n \geq 4$ pooled mice/group and $n \geq 3$ experimental replicates/group.
774 ns, not significant. **** $p < 0.0001$. 2way ANOVA test comparing D21PBS NKs and D21SPN
775 NKs values in each condition.
776
777 **Figure S1:**
778
779 **(A)** Representative contour plots for NK cell purity of D21PBS (black symbols) and D21SPN
780 (red symbols) samples based on NK1.1$^+$ CD3$^-$ or NK1.1$^+$ DX5$^+$ markers (**left panel**). Percentage
781 of NK cells among live cells (purity of cells, **right panel**). Box plots where each dot represents
782 a pool of mice from one experiment, lines are the median, error bars show min to max. Data
783 are representative of more than three repeats with $n \geq 4$ pooled mice/group.
784 **(B)** Mouse infections are carried out as in the scheme in Figure 1A. NK cells were isolated from
785 spleens of mice previously infected with *S. pneumoniae* (red bars, D21SPN NKs) or not (black
786 bars, D21PBS NKs). Highly purified NK cells were fixed, and chromatin was extracted and
787 sheared. ChIP for H3K4me1 were performed and resulting positive fractions of the chromatin
788 were amplified using PCR for the indicated targets. Enrichment percentage for H3K4me1 pull-

789 down on regions upstream the *ifng* gene in NK cells from D21PBS and D21SPN mice. Data
790 are representative of four experiments with n ≥ 4 mice/group.
791 **(C-D)** Splenocytes were harvested from mice 12 days **(B)** or 21 days **(C)** after they were
792 intranasally injected with either PBS (black symbols) or sub-lethal dose of *S. pneumoniae* (SPN,
793 red symbols, 5.10^5 CFU) for two consecutive days. NK cell expression of several NK cell
794 receptors in percentages (**left panel**) and intensity of expression (MFI, **right panel**). Box plots
795 where each dot represents an individual mouse, lines are the median, error bars show min to
796 max. Data are pooled from one **(B)** or two **(C)** repeats with n ≥ 4 mice/group.
797 ns, not significant. * $p < 0.05$ and ** $p < 0.01$. Mann-Whitney **(A,B)** and 2way ANOVA **(C,D)**
798 tests for statistical significance.
799
800 **Figure 2: Sub-lethal infection with *S. pneumoniae* induces a rapid and transient immune**
801 **response that returns to basal state before 21 days.**
802
803 **(A)** Experimental scheme, showing that C57BL/6 mice were intranasally injected with either
804 PBS (black symbols) or sub-lethal dose of *S. pneumoniae* (SPN, red symbols, 5.10^5 CFU) for
805 two consecutive days. Organs were collected at 24h, 72h and 21 days post-infection for CFU
806 counts and cellular infiltrate determination by flow cytometry.
807 **(B-D)** Organs were collected at 24h (**B**), 72h (**C**) and 21 days post-infection (**D**). CFU counts
808 in the nasal lavage, BALF, lungs, spleen and blood of infected mice (**left panel**). Box plots
809 where each dot represents an individual mouse, lines are the mean, error bars show min to max
810 and dotted lines represent limit of detection. Percentage of neutrophils ($CD11b^+$ $Ly6G^+$) among
811 $CD45^+$ cells in the lungs and bronchio-alveolar lavage fluid (BALF), percentage of $CD69^+$
812 neutrophils in the BALF (**middle panel**). Percentage of NK cells ($NK1.1^+$ $CD3^-$) among $CD45^+$
813 cells, percentage of IFNγ^+, $Perforin^+$, Granzyme B^+ NK cells in the lungs and spleen (**right**

814 **panel**). Box plots where each dot represents an individual mouse (black dots for uninfected
815 mice, red dots for infected mice), lines are the median, error bar show min to max.
816 Data are pooled from one, two or three repeats with n ≥ 3 mice/group. ns, not significant. * p <
817 0.05 and ** p <0.01, Mann-Whitney test for single comparisons and 2way ANOVA test for
818 multiple comparisons.
819
820 **Figure S2**
821
822 Weight **(A)** and clinical score **(B)** following the infection scheme from Figure 2A. Dots
823 represent the mean and error bars are the standard error of the mean (SEM). Data are pooled
824 from two repeats with n = 4 mice/group.
825 **(C-E)** Organs were collected at 24h (**C**), 72h (**D**) and 21 days post-infection (**E**). Absolute
826 numbers of neutrophils ($CD11b^+$ $Ly6G^+$) in the lungs and bronchio-alveolar lavage fluid
827 (BALF) (**left panel**). Absolute numbers of NK cells ($NK1.1^+$ $CD3^-$), percentage of $CD69^+$ NK
828 cells, intensity of Granzyme B expression (MFI) and representative overlay histogram of
829 Granzyme B staining in NK cells (**right panel**). Box plots where each dot represents an
830 individual mouse (black dots for uninfected mice, red dots for infected mice), lines are the
831 median, error bar show min to max. Grey histogram represents isotype control. Data are pooled
832 from one, two or three repeats with n ≥ 4 mice/group.
833 ns, not significant. * p < 0.05. Mann-Whitney test for statistical significance.
834
835 **Figure 3: Transferred memory NK cells protect mice from lethal *S. pneumoniae* infection**
836 **for at least 12 weeks.**
837

(A) Experimental scheme. C57BL/6 mice (donor mice) were intranasally injected with either PBS (black symbols) or sub-lethal dose of *S. pneumoniae* (SPN, red symbols, 5.10^5 CFU) for two consecutive days. After 21 days or 12 weeks, NK cells from spleens were highly purified (98%) and transferred into naïve mice (recipient mice, intravenously, 2.10^5 cells). One day after, all recipient mice were intranasally infected with a lethal dose of *S. pneumoniae* (5.10^6 CFU for survival study, 1.10^7 CFU for bacterial counts comparison) or *L. monocytogenes* (1.10^6 CFU, intravenously). Organs were collected at 24h and 40h post-infection for CFU counts and flow cytometry analysis.

(B) Bacterial counts at 40h post-infection in the nasal lavage, bronchio-alveolar lavage fluid (BALF), lungs, blood and spleen of mice having received either D21PBS NKs (black symbols) or D21SPN NKs (red symbols). Box plots where each dot represents an individual mouse, lines are the mean, error bars show min to max and dotted lines represent limit of detection. Data are pooled from at least three repeats with $n \geq 3$ mice/group.

(C) Survival curve. Dots represent the percentage of survival of total mice. Data are representative of two repeats with $n = 4$ mice/group.

(D) Clinical score. Dots represent the mean, error bars show the standard error of the mean (SEM). Data are representative of two repeats with $n = 4$ mice/group.

(E) Weight represented as percentage of initial body weight loss. Dots represent the mean, error bars show the standard error of the mean (SEM). After death, mice have the value of 80%. Data are representative of two repeats with $n = 4$ mice/group.

(F) Bacterial counts at 40h post-infection in the lungs and spleen of mice having received either W12PBS NKs (black symbols) or W12SPN NKs (red symbols). Box plots where each dot represents an individual mouse, lines are the mean, error bars show min to max and dotted lines represent limit of detection. Data are pooled from three repeats with $n \geq 4$ mice/group

(G) Bacterial counts at 40h post-infection in the spleen and liver of mice infected with *Listeria monocytogenes* (intravenously) and having previously received either D21PBS NKs (black symbols) or D21SPN NKs (red symbols). Box plots where each dot represents an individual mouse, lines are the mean, error bars show min to max and dotted lines represent limit of detection. Data are pooled from two repeats with n = 3 mice/group.

ns, not significant. * $p < 0.05$, ** $p < 0.01$, *** $p < 0.001$ **** $p < 0.0001$. 2way ANOVA **(B),** Log-rank (Mantel-Cox) **(C)** and Mann-Whitney **(F, G)** tests for statistical significance.

Figure S3

(A-B) Mouse infections are carried out as in the scheme in Figure 3A. Congenic mice are used to distinguish donor NK cells ($CD45.2^+$) from recipient NK cells ($CD45.1^+$).

(A) Representative gating strategy to measure purity of transferred D21PBS NKs (black symbols) or D21SPN NKs (red symbols) in the lungs of recipient mice at 24 hours post-infection. Purity represents the percentage of NK cells among $CD45.2^+$ transferred cells. Box plots where each dot represents an individual recipient mouse, lines are the median, error bar show min to max. Data are representative of three repeats with $n \geq 4$ mice/group.

(B) Representative gating strategy to detect transferred NK cells. Percentages and numbers of $CD45.2^+$ transferred NK cells in the lungs and blood of CD45.1 recipient mice at 24h and 40h post-infection. Box plots where each dot represents an individual recipient mouse, lines are the median, error bar show min to max. Data are pooled from at least two repeats with $n \geq 3$ mice/group.

ns, not significant. Mann-Whitney test for statistical significance.

Figure 4: Protection of mice mediated by memory NK cells is IFNγ independent.

887

888 **(A-B)** Mouse infections are carried out as in the scheme in Figure 3A. Organs were collected
889 at 24h and 40h post-infection for flow cytometry analysis and ELISA assays.
890 **(A)** Flow cytometry analysis of IFNγ expression in CD45.1$^+$ endogenous NK cells and CD45.2$^+$
891 transferred NK cells (hatched) into both mice having received D21PBS NK cells (black) and
892 mice having received D21SPN NK cells (red). Violin plot where each dot represents an
893 individual mouse, lines are the median. Data are pooled from two repeats with n ≥ 2 mice/group.
894 **(B)** IFNγ ELISA assays of lung supernatants from infected mice having received either
895 D21PBS NKs (black) or D21SPN NKs (red) at 24h and 40h post-infection. Bars are the mean
896 of at least four experiments with n ≥ 4 mice/group, each dot represents an individual mouse and
897 error bars are the standard error of the mean (SEM).
898 **(C)** Mouse infections are carried out as in the scheme in Figure 3A, with the exception that WT
899 mice were used as donor mice and Ifngr KO mice as recipient mice. Bacterial counts at 40h
900 post-infection in the lungs and spleen of Ifngr KO mice having received D21PBS WT NK cells
901 (black symbols) or D21SPN WT NK cells (red symbols). Box plots where each dot represents
902 an individual mouse, lines are the mean, error bars show min to max and dotted lines represent
903 limit of detection. Data are pooled from two repeats with n ≥ 4 mice/group.
904 **(D)** WT and Ifngr KO mice were intranasally infected with a lethal dose of *S. pneumoniae*
905 (1.10^7 CFU). Lungs were collected at 40h post-infection for CFU counts and flow cytometry
906 analysis. Percentages of neutrophils (Ly6G$^+$ CD11b$^+$), NK cells (NK1.1$^+$ CD3$^-$) and CD69$^+$ NK
907 cells. Box plots where each dot represents an individual mouse, lines are the mean, error bars
908 show min to max and dotted lines represent limit of detection. Data are pooled from two repeats
909 with n ≥ 3 mice/group
910 ns, not significant. * $p < 0.05$, ** $p < 0.01$. 2way ANOVA **(A,B)** and Mann-Whitney **(C,D)**
911 tests for statistical significance.

Figure 5: Protection of mice appears to be an intrinsic NK cell property.

Mouse infections are carried out as in the scheme in Figure 3A. Organs were collected at 24h and 40h post-infection for flow cytometry analysis, ELISA assays and CFU counts.

(A) Cellular infiltrate analysis in the lungs at 24h post-infection. Percentage of respective cell types among $CD45^+$ cells (**left panel**) and absolute number of cells for each cell type (**right panel**): neutrophils ($Ly6G^+$ $CD11b^+$), alveolar macrophages (AM) ($Ly6G^-$ $SiglecF^+$ $CD64^+$ $CD11b^-$), interstitial macrophages (IM) ($Ly6G^-$ $SiglecF^-$ $CD11b^{high}$ $MHCII^+$ $CD64^+$ $CD24^-$), monocytes ($Ly6G^-$ $SiglecF^-$ $CD11b^{high}$ $MHCII^-$), eosinophils ($Ly6G^-$ $SiglecF^+$ $CD11b^+$), dendritic cells (DCs) ($CD103^+$ DCs : $Ly6G^-$ $SiglecF^-$ $CD11b^{low}$ $CD103^+$ $CD24^+$ + $CD11b^+$ DCs : $Ly6G^-$ $SiglecF^-$ $CD11b^{high}$ $MHCII^+$ $CD64^-$ $CD24^+$), NK cells ($NK1.1^+$ $CD3^-$), T cells ($NK1.1^-$ $CD3^+$). Radar plots with each value representing the geometric mean of three repeats with n = 4 mice. The blue line for uninfected mice, black line for mice having received D21PBS NKs and red line for mice having received D21SPN NKs.

(B) Cellular infiltrate analysis in the bronchio-alveolar lavage fluid (BALF) at 24h post-infection. Percentage of respective cell types among $CD45^+$ cells (**left panel**) and absolute number of cells for each cell type (**right panel**): neutrophils ($Ly6G^+$ $CD11b^+$), alveolar macrophages ($SiglecF^+$ $CD64^+$ $CD11b^-$). Box plots where each dot represents an individual mouse (blue dots for uninfected mice, black dots for mice having received D21PBS NKs, red dots for mice having received D21SPN NKs), lines are the median, error bar show min to max. Date are pooled from at least two repeats with $n \geq 2$ mice/group.

(C) Cellular activation analysis in the lung at 40h post-infection. Percentages of $CD69^+$ neutrophils, $CD69^+$ NK cells and $CD86^+$ interstitial macrophages. Box plots where each dot represents an individual mouse (the blue dots are for uninfected mice, black dots for mice

having received D21PBS NKs, red dots for mice having received D21SPN NKs), lines are the median, error bar show min to max. Data are pooled from two repeats with n ≥ 1 mice/group.

(D) ELISA assays of lung supernatants from infected mice at 40h post-infection. Bars are the mean of at least 3 experiments with n ≥ 3 mice/group, error bars are the standard error of the mean (SEM).

(E-F) At 40h post-infection, lung supernatants of mice having received either D21PBS NKs (black) or D21SPN NKs (red) **(C) -** either We12PBS NKs (black) or We12SPN NKs (red) **(D)** were collected to perform Granzyme B ELISA assays. Bars are the mean of at least three experiments with n ≥ 3 mice/group, each dot represents an individual mouse and error bars are the standard error of the mean (SEM).

ns, not significant. * $p < 0.05$, ** $p < 0.01$, *** $p < 0.001$. Kruskal-Wallis **(A,B,C)**, 2way ANOVA **(D)** and Mann-Whitney **(E,F)** tests for statistical significance.

Figure S4

Mouse infections are carried out as in the scheme in Figure 3A. Organs were collected at 24h and 40h post-infection for flow cytometry analysis and ELISA assays.

(A) Gating strategy used to identify myeloid-cell subsets in the lungs at 24h post-infection, adapted from Misharin et al. 2013. After the exclusion of debris, doublets and dead cells, immune cells were identified by CD45 staining. Neutrophils, alveolar macrophages and eosinophils are defined with the following specific markers respectively: $Ly6G^+$ $CD11b^+$, $SiglecF^+$ $CD11b^-$, $SiglecF^+$ $CD11b^+$. Gating on $CD11b^{high}$ was used to distinguish myeloid cells from lymphoid cells with the exception of $CD103^+$ dendritic cells that are defined as $CD11b^{low}$ $CD103^+$ $CD24^+$ cells. In $CD11b^{high}$ subset, gating on $MHCII^+$ cells allow to identify interstitial macrophages as $MHCII^+$ $CD64^+$ $CD24^-$ cells and $CD11b^+$ dendritic cells as $MHCII^+$ $CD64^-$

962 $CD24^+$ cells. On the contrary, $CD11b^{high}$ $MHCII^-$ cells are monocytes/immature macrophages
963 that can have different maturation states based on Ly6C marker.
964 **(B)** Cellular activation analysis in the lungs at 40h post-infection. Intensity of CD11b
965 expression in neutrophils (MFI), percentage of ROS^+ neutrophils and intensity of MHCII
966 expression in interstitial macrophages (MFI). Box plots with each dot representing individual
967 mice (blue dots for uninfected mice, black dots for mice having received D21PBS NKs, red
968 dots for mice having received D21SPN NKs), lines are the median, error bar show min to max.
969 Data are pooled from two repeats with $n \geq 1$ mice/group.
970 **(C)** ELISA assays of lung supernatants from infected mice having received either D21PBS NKs
971 (black) or D21SPN NKs (red) at 24h post-infection. Bars are the mean of at least 3 experiments
972 with $n \geq 3$ mice/group, error bars are the standard error of the mean (SEM).
973 **(D)** Granzyme B ELISA assays of lung supernatants from infected mice having received either
974 D21PBS NKs (black) or D21SPN NKs (red) at 24h post-infection. Bars are the mean of at least
975 3 experiments with $n \geq 3$ mice/group, error bars are the standard error of the mean (SEM).
976 ns, not significant. Kruskal-Wallis **(B)**, 2way ANOVA **(C)** and Mann-Whitney **(D)** tests for
977 statistical significance.
978
979 **Figure 6: Cytotoxic proteins are upregulated by memory NK cells and important for**
980 **protection of mice.**
981 **(A-B)** C57BL/6 mice were intranasally injected with either PBS (black symbols) or sub-lethal
982 dose of *S. pneumoniae* (SPN, red symbols, 5.10^5 CFU) for two consecutive days. After 21 days,
983 NK cells were highly purified from spleens of D21PBS or D21SPN mice (98% of purity) and
984 stimulated *in vitro* with cytokines (IL-15 at 2 ng/ml, IL-18 at 1,5 ng/ml, IL-12 at 1,25 ng/ml)
985 and formaldehyde inactivated bacteria (MOI 20) for 24 hours.
986 SPN : *S. pneumoniae*, GBS : *S. agalactiae,* Listeria : *L. monocytogenes*.

(A) Intensity of Granzyme B expression in NK cells (MFI, **left panel**), percentage of Granzyme B^+ NK cells (**middle panel**), representative overlay histogram upon IL-15+IL-18+SPN stimulation (**right panel**, gray represents isotype control). Box plots where each dot represents a pool of mice from one experiment (black dots for D21PBS NKs, red dots for D21SPN NKs), line are median, error bar show min to max. Data are representative at least one experiment with $n \geq 4$ pooled mice/group and $n \geq 3$ experimental replicates/group.

(B) Intensity of Perforin expression in NK cells (MFI, **left panel**), percentage of $Perforin^+$ NK cells (**middle panel**), representative overlay histogram upon IL-15+IL-18+SPN stimulation (**right panel**, gray represents isotype control). Box plots where each dot represents a pool of mice from one experiment (black dots for D21PBS NKs, red dots for D21SPN NKs), line are median, error bar show min to max. Data are representative of at least one experiments with $n \geq 4$ pooled mice/group and $n \geq 3$ experimental replicates/group.

(C) Mouse infections are carried out as in the scheme in Figure 3A, with the exception that Prf1 KO mice were used as both donor and recipient mice. Bacterial counts at 40h post-infection in the nasal lavage, bronchio-alveolar lavage fluid (BALF), lungs and spleen of Prf1 KO mice having received D21PBS Prf1 KO NK cells (black symbols) or D21SPN Prf1 KO NK cells (red symbols). Box plots where each dot represents an individual mouse, lines are the mean, error bars show min to max and dotted lines represent limit of detection. Data are pooled from two repeats with $n \geq 3$ mice/group.

ns, not significant. * $p < 0.05$, *** $p < 0.001$. 2way ANOVA **(A,B)** and Mann-Whitney **(C)** tests for statistical significance.

Figure S5

(A) Mouse infections are carried out as in the scheme in Figure 1A. NK cells were isolated from spleens of mice previously infected with *S. pneumoniae* (red bars, D21SPN NKs) or not

(black bars, D21PBS NKs). Highly purified NK cells were fixed, and chromatin was extracted and sheared. ChIP for H3K4me1 were performed and resulting positive fractions of the chromatin were amplified using PCR for the indicated targets. Enrichment percentage for H3K4me1 pull-down on -34kb upstream the *gzmb* gene and intergenic regions (IG) in NK cells from D21PBS and D21SPN mice. Data are representative of at least three experiments with n ≥ 4 mice/group.

(B) Mouse infections and *in vitro* experiments are carried out as in the scheme in Figure 1A, with the exception that Prf1 KO mice were used. Purified D21PBS (black) or D21SPN (red) Prf1 KO NK cells were stimulated *in vitro* with cytokines (IL-15 at 2 ng/ml and IL-18 at 1,5 ng/ml) and formaldehyde inactivated *S. pneumoniae* (SPN, MOI 20) for 24 hours. Intensity of Granzyme B expression in NK cells (MFI, **left panel**) and percentage of Granzyme B^+ NK cells (**right panel**) upon *in vitro* stimulation. Box plots where each dot represents a pool of mice from one experiment, lines are median, error bar show min to max. Data are representative of one experiment with n = 4 pooled mice/group and n ≥ 2 experimental replicates/group.

(C-D) Mouse infections and *in vivo* transfers are carried out as in the scheme in Figure 3A, with the exception that Prf1 KO mice were used as both donor and recipient mice.

(C) Granzyme B ELISA experiment of lung supernatants from infected mice at 40h post-infection, having received either D21PBS (black) or D21SPN (red) Prf1 KO NK cells. Dots represent individual mice, bars are the mean and error bars are the standard error of the mean (SEM). Data are representative of one experiment with n ≥ 3 mice/group.

(D) Percentages of neutrophils, $CD69^+$ neutrophils and NK cells in the lungs of Prf1 KO recipient mice having received either D21PBS (black) or D21SPN (red) Prf1 KO NK cells. Box plots with each dot representing individual mice, lines are the median, error bar show min to max. Data are representative of one experiment with n ≥ 3 mice/group.

ns, not significant. Mann-Whitney tests for statistical significance.

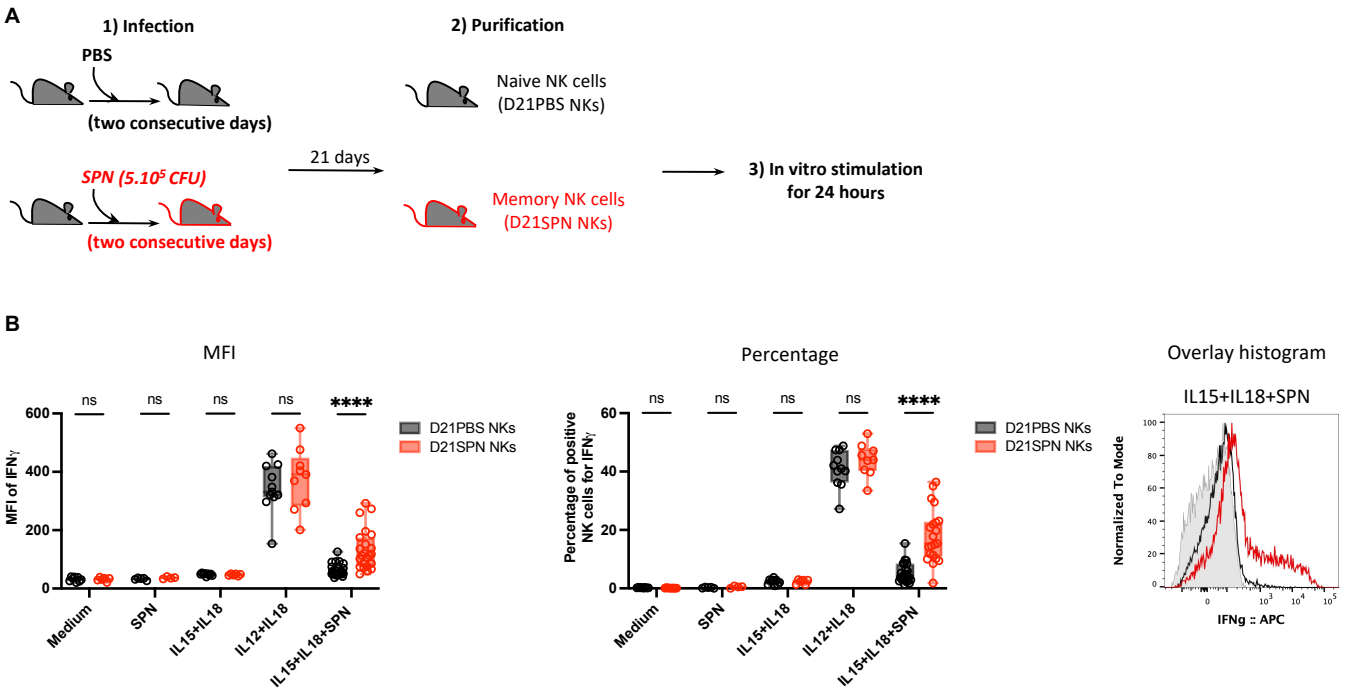

Figure 1: NK cells acquire intrinsic memory features 21 days after *in vivo* infection

(A) Experimental scheme. C57BL/6 mice were intranasally injected with either PBS (black symbols) or sub-lethal dose of *S. pneumoniae* (SPN, red symbols, 5.10^5 CFU) for two consecutive days. After 21 days, NK cells were highly purified from spleens of D21PBS or D21SPN mice (98% of purity) and stimulated *in vitro* with cytokines (IL-15 at 2 ng/ml, IL-18 at 1,5 ng/ml, IL-12 at 1,25 ng/ml) and formaldehyde inactivated *S. pneumoniae* (SPN, MOI 20) for 24 hours.
(B) Intensity of IFNγ expression in NK cells (MFI, **left panel**), percentage of IFNγ^+ NK cells (**middle panel**), representative overlay histogram upon IL-15+IL-18+SPN stimulation (**right panel**, gray represents isotype control). Box plots where each dot represents a pool of mice from one experiment (black dots for D21PBS NKs, red dots for D21SPN NKs), lines are median, error bars show min to max. Data are representative of at least three experiments with $n \geq 4$ pooled mice/group and $n \geq 3$ experimental replicates/group.
ns, not significant. **** $p < 0.0001$. 2way ANOVA test comparing D21PBS NKs and D21SPN NKs values in each condition.

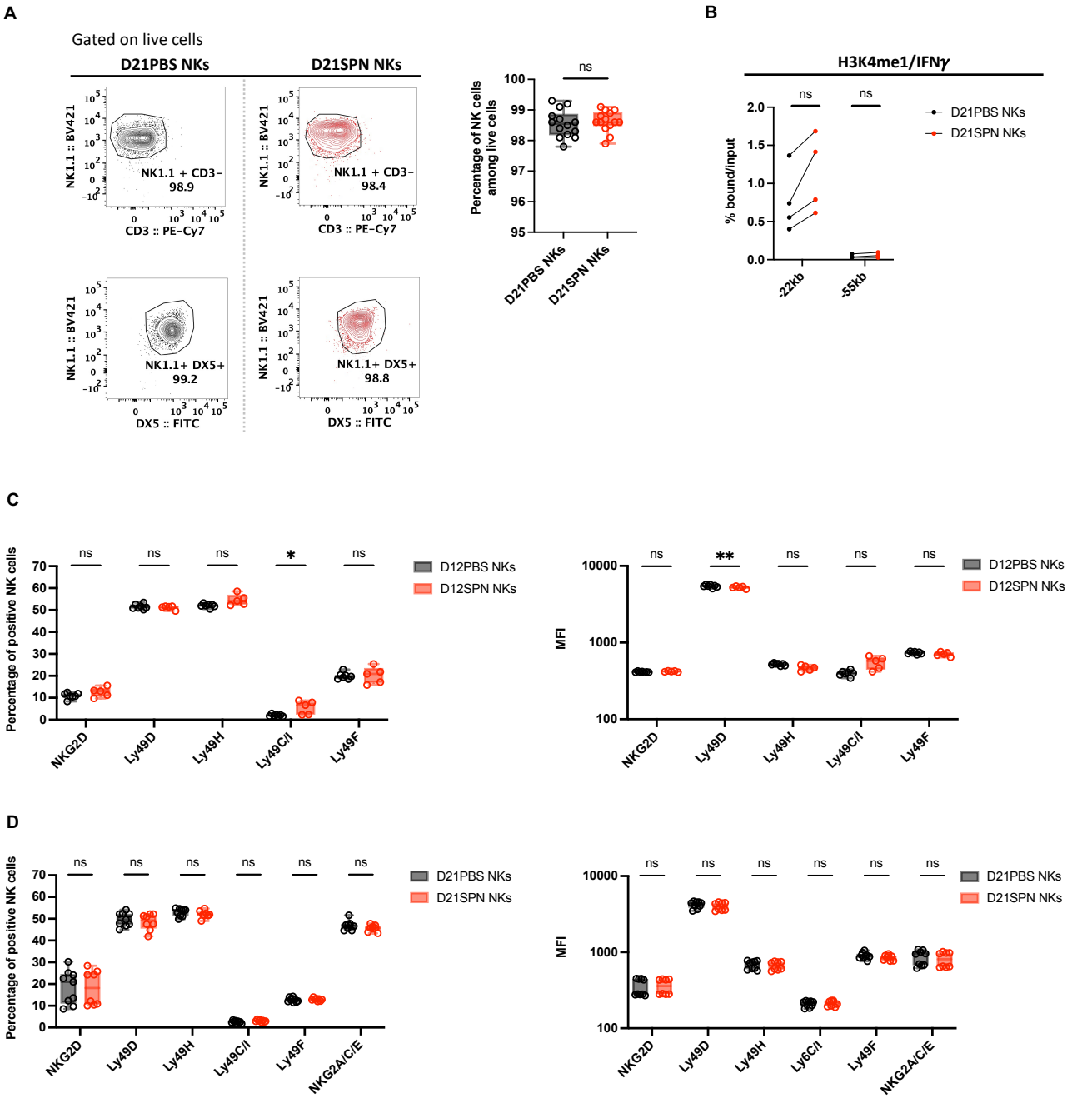

Figure S1:

(A) Representative contour plots for NK cell purity of D21PBS (black symbols) and D21SPN (red symbols) samples based on NK1.1$^+$ CD3$^-$ or NK1.1$^+$ DX5$^+$ markers (**left panel**). Percentage of NK cells among live cells (purity of cells, **right panel**). Box plots where each dot represents a pool of mice from one experiment, lines are the median, error bars show min to max. Data are representative of more than three repeats with n ≥4 pooled mice/group and n ≥ 3 experimental replicates/group.

(B) Mouse infections are carried out as in the scheme in Figure 1A. NK cells were isolated from spleens of mice previously infected with *S. pneumoniae* (red bars, D21SPN NKs) or not (black bars, D21PBS NKs). Highly purified NK cells were fixed, and chromatin was extracted and sheared. ChIP for H3K4me1 were performed and resulting positive fractions of the chromatin were amplified using PCR for the indicated targets. Enrichment percentage for H3K4me1 pull-down on regions upstream the *ifng* gene in NK cells from D21PBS and D21SPN mice. Data are representative of four experiments with n ≥ 4 mice/group.

(C-D) Splenocytes were harvested from mice 12 days **(C)** or 21 days **(D)** after they were intranasally injected with either PBS (black symbols) or sub-lethal dose of *S. pneumoniae* (SPN, red symbols, 5.10^5 CFU) for two consecutive days. NK cell expression of several NK cell receptors in percentages (**left panel**) and intensity of expression (MFI, **right panel**). Box plots where each dot represents an individual mouse, lines are the median, error bars show min to max. Data are pooled from one **(C)** or two **(D)** repeats with n ≥ 4 mice/group.

ns, not significant. * p < 0.05 and ** p <0.01. Mann-Whitney **(A,B)** and 2way ANOVA **(C,D)** tests for statistical significance.

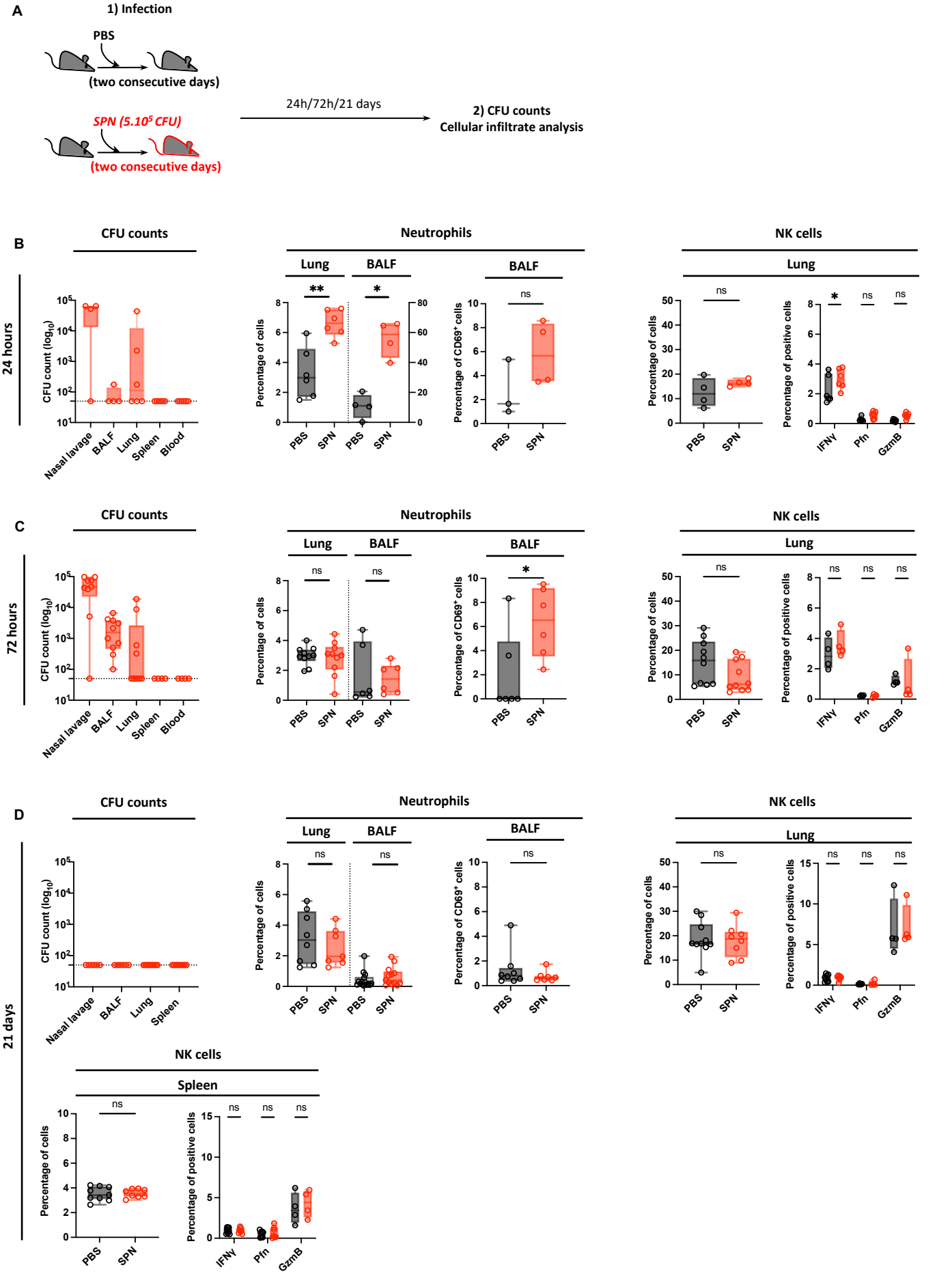
A
1) Infection
PBS
(two consecutive days)
SPN (5.10⁵ CFU)
(two consecutive days)
24h/72h/21 days
2) CFU counts
Cellular infiltrate analysis
B
24 hours
CFU counts
CFU count (log10)
Nasal lavage
BALF
Lung
Spleen
Blood
Neutrophils
Lung
BALF
BALF
Percentage of cells
Percentage of CD69+ cells
PBS
SPN
NK cells
Lung
Percentage of cells
Percentage of positive cells
IFNγ
Pfn
GzmB
ns
C
72 hours
D
21 days
Spleen

Figure 2: Sub-lethal infection with *S. pneumoniae* induces a rapid and transient immune response that returns to basal state before 21 days

(A) Experimental scheme, showing that C57BL/6 mice were intranasally injected with either PBS (black symbols) or sub-lethal dose of *S. pneumoniae* (SPN, red symbols, 5.10^5 CFU) for two consecutive days. Organs were collected at 24h, 72h and 21 days post-infection for CFU counts and cellular infiltrate determination by flow cytometry.
(B-D) Organs were collected at 24h (**B**), 72h (**C**) and 21 days post-infection (**D**). CFU counts in the nasal lavage, BALF, lungs, spleen and blood of infected mice (**left panel**). Box plots where each dot represents an individual mouse, lines are the mean, error bars show min to max and dotted lines represent limit of detection. Percentage of neutrophils ($CD11b^+$ $Ly6G^+$) among $CD45^+$ cells in the lungs and bronchio-alveolar lavage fluid (BALF), percentage of $CD69^+$ neutrophils in the BALF (**middle panel**). Percentage of NK cells ($NK1.1^+$ $CD3^-$) among $CD45^+$ cells, percentage of IFNγ^+, $Perforin^+$, Granzyme B^+ NK cells in the lungs and spleen (**right panel**). Box plots where each dot represents an individual mouse (black dots for uninfected mice, red dots for infected mice), lines are the median, error bar show min to max.
Data are pooled from one, two or three repeats with $n \geq 3$ mice/group. ns, not significant. * $p < 0.05$ and ** $p < 0.01$, Mann-Whitney test for single comparisons and 2way ANOVA test for multiple comparisons.

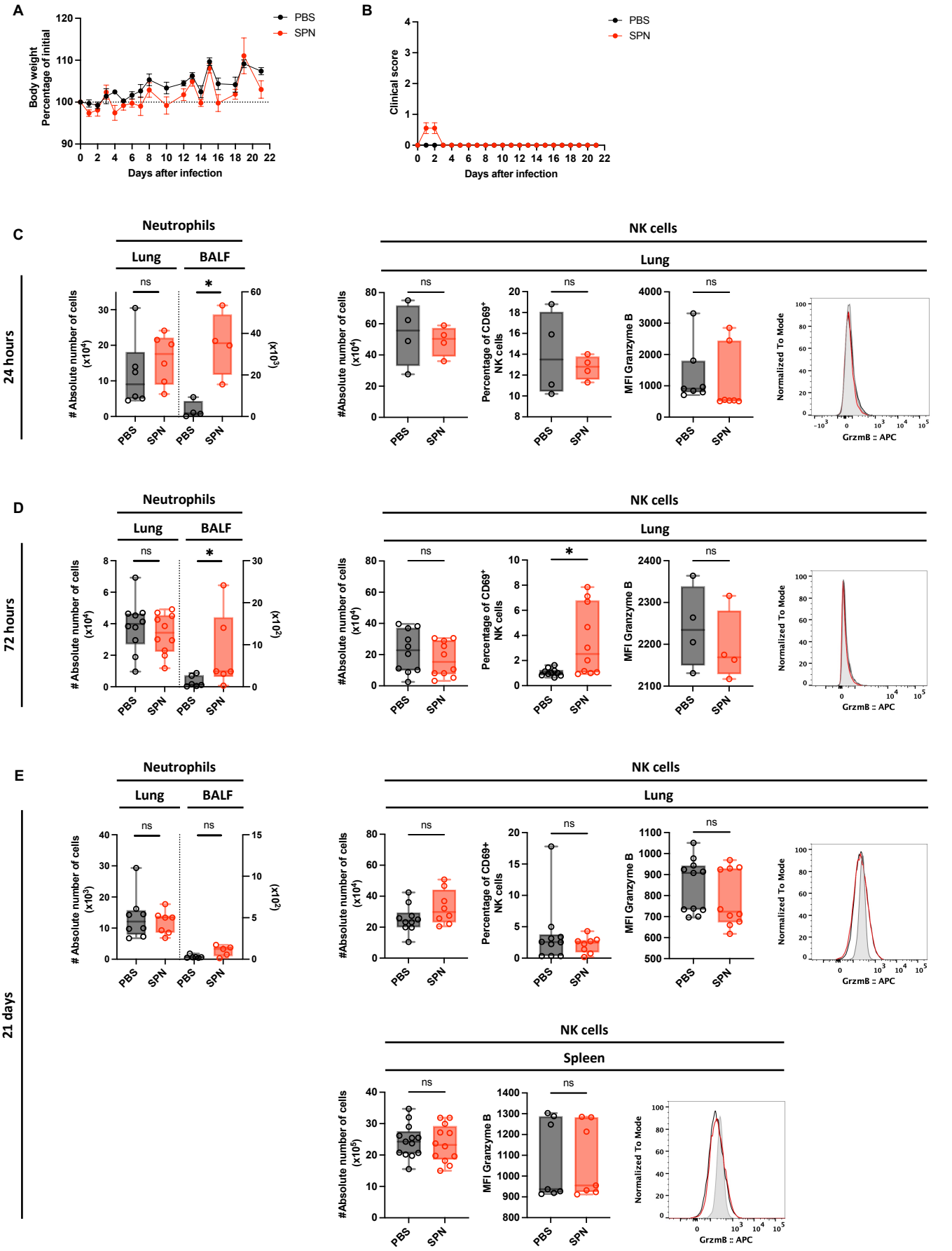
A
Body weight Percentage of initial
Days after infection
PBS
SPN
B
Clinical score
Days after infection
C
24 hours
Neutrophils
Lung
BALF
Absolute number of cells (x10⁴)
(x10³)
NK cells
Lung
#Absolute number of cells (x10⁴)
Percentage of CD69⁺ NK cells
MFI Granzyme B
Normalized To Mode
GrzmB :: APC
D
72 hours
E
21 days
Spleen
#Absolute number of cells (x10⁵)
ns

Figure S2

Weight **(A)** and clinical score **(B)** following the infection scheme from Figure 2A. Dots represent the mean and error bars are the standard error of the mean (SEM). Data are pooled from two repeats with n = 4 mice/group

(C-E) Organs were collected at 24h (**C**), 72h (**D**) and 21 days post-infection (**E**). Absolute numbers of neutrophils ($CD11b^+$ $Ly6G^+$) in the lungs and bronchio-alveolar lavage fluid (BALF) (**left panel**). Absolute numbers of NK cells ($NK1.1^+$ $CD3^-$), percentage of $CD69^+$ NK cells, intensity of Granzyme B expression (MFI) and representative overlay histogram of Granzyme B staining in NK cells (**right panel**). Box plots where each dot represents an individual mouse (black dots for uninfected mice, red dots for infected mice), lines are the median, error bar show min to max. Grey histogram represents isotype control. Data are pooled from one, two or three repeats with $n \geq 4$ mice/group.

ns, not significant. * $p < 0.05$. Mann-Whitney test for statistical significance.

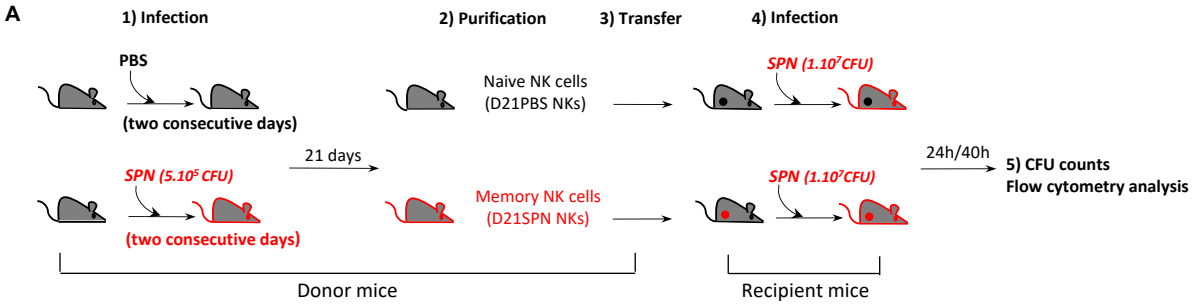
A
1) Infection
PBS
(two consecutive days)
2) Purification
3) Transfer
4) Infection
Naive NK cells
(D21PBS NKs)
SPN (1.10⁷CFU)
21 days
SPN (5.10⁵ CFU)
(two consecutive days)
Memory NK cells
(D21SPN NKs)
SPN (1.10⁷CFU)
24h/40h
5) CFU counts
Flow cytometry analysis
Donor mice
Recipient mice

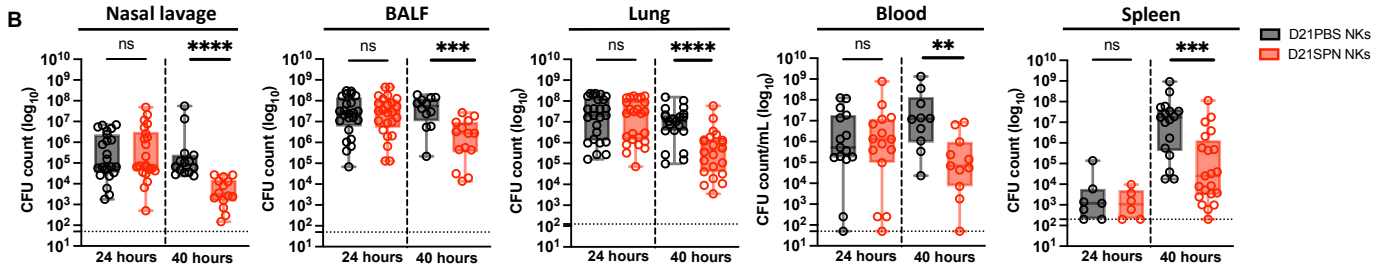
B
Nasal lavage
BALF
Lung
Blood
Spleen
ns
****
***
**
CFU count (log10)
CFU count/mL (log10)
24 hours
40 hours
D21PBS NKs
D21SPN NKs

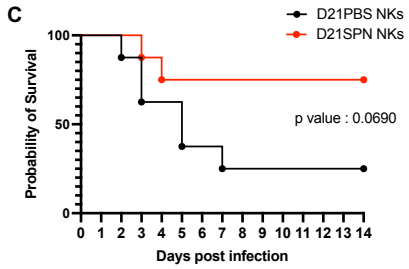
C
D21PBS NKs
D21SPN NKs
Probability of Survival
p value : 0.0690
Days post infection

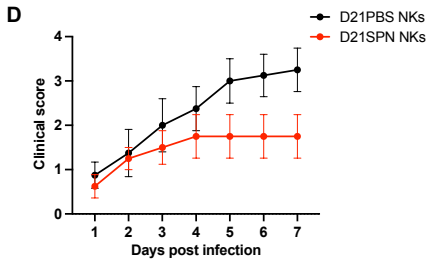
D
D21PBS NKs
D21SPN NKs
Clinical score
Days post infection

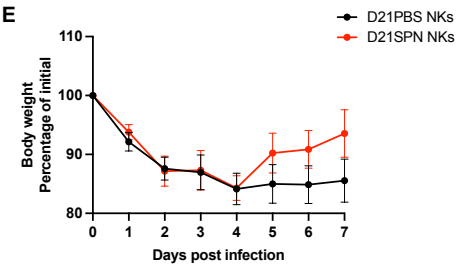
E
D21PBS NKs
D21SPN NKs
Body weight
Percentage of initial
Days post infection

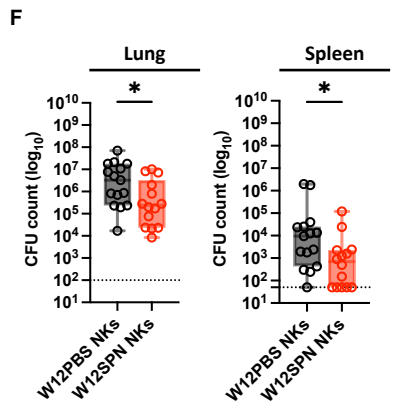
F
Lung
Spleen
*
CFU count (log10)
W12PBS NKs
W12SPN NKs

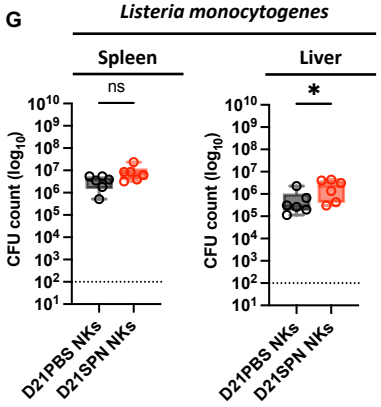
G
Listeria monocytogenes
Spleen
Liver
ns
*
CFU count (log10)
D21PBS NKs
D21SPN NKs

Figure 3: Transferred memory NK cells protect mice from lethal *S. pneumoniae* infection for at least 12 weeks

(A) Experimental scheme. C57BL/6 mice (donor mice) were intranasally injected with either PBS (black symbols) or sub-lethal dose of *S. pneumoniae* (SPN, red symbols, 5.10^5 CFU) for two consecutive days. After 21 days or 12 weeks, NK cells from spleens were highly purified (98%) and transferred into naïve mice (recipient mice, intravenously, 2.10^5 cells). One day after, all recipient mice were intranasally infected with a lethal dose of *S. pneumoniae* (5.10^6 CFU for survival study, 1.10^7 CFU for bacterial counts comparison) or *L. monocytogenes* (1.10^6 CFU, intravenously). Organs were collected at 24h and 40h post-infection for CFU counts and flow cytometry analysis.
(B) Bacterial counts at 40h post-infection in the nasal lavage, bronchio-alveolar lavage fluid (BALF), lungs, blood and spleen of mice having received either D21PBS NKs (black symbols) or D21SPN NKs (red symbols). Box plots where each dot represents an individual mouse, lines are the mean, error bars show min to max and dotted lines represent limit of detection. Data are pooled from at least two repeats with $n \geq 3$ mice/group.
(C) Survival curve. Dots represent the percentage of survival of total mice. Data are representative of two repeats with $n = 4$ mice/group.
(D) Clinical score. Dots represent the mean, error bars show the standard error of the mean (SEM). Data are representative of two repeats with $n = 4$ mice/group.
(E) Weight represented as percentage of initial body weight loss. Dots represent the mean, error bars show the standard error of the mean (SEM). After death, mice have the value of 80%. Data are representative of two repeats with $n = 4$ mice/group.
(F) Bacterial counts at 40h post-infection in the lungs and spleen of mice having received either W12PBS NKs (black symbols) or W12SPN NKs (red symbols). Box plots where each dot represents an individual mouse, lines are the mean, error bars show min to max and dotted lines represent limit of detection. Data are pooled from three repeats with $n \geq 4$ mice/group
(G) Bacterial counts at 40h post-infection in the spleen and liver of mice infected with *Listeria monocytogenes* (intravenously) and having previously received either D21PBS NKs (black symbols) or D21SPN NKs (red symbols). Box plots where each dot represents an individual mouse, lines are the mean, error bars show min to max and dotted lines represent limit of detection. Data are pooled from two repeats with $n = 3$ mice/group.
ns, not significant. * $p < 0.05$, ** $p < 0.01$, *** $p < 0.001$ **** $p < 0.0001$. 2way ANOVA **(B),** Log-rank (Mantel-Cox) **(C)** and Mann-Whitney **(F, G)** tests for statistical significance.

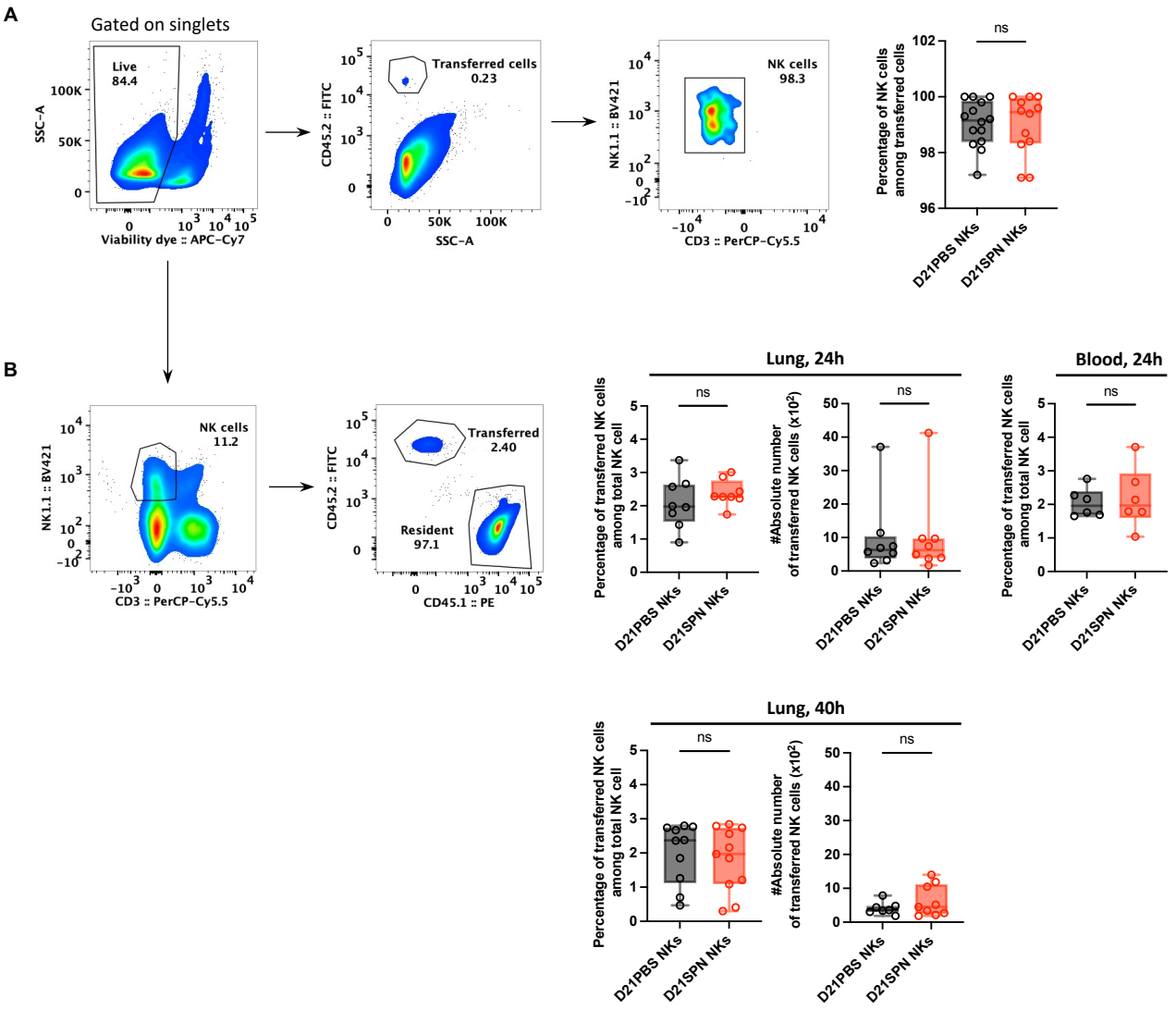

Figure S3

(A-B) Mouse infections are carried out as in the scheme in Figure 3A. Congenic mice are used to distinguish donor NK cells ($CD45.2^+$) from recipient NK cells ($CD45.1^+$).

(A) Representative gating strategy to measure purity of transferred D21PBS NKs (black symbols) or D21SPN NKs (red symbols) in the lungs of recipient mice at 24 hours post-infection. Purity represents the percentage of NK cells among $CD45.2^+$ transferred cells. Box plots where each dot represents an individual recipient mouse, lines are the median, error bar show min to max. Data are representative of three repeats with $n \geq 4$ mice/group.

(B) Representative gating strategy to detect transferred NK cells. Percentages and numbers of $CD45.2^+$ transferred NK cells in the lungs and blood of CD45.1 recipient mice at 24h and 40h post-infection. Box plots where each dot represents an individual recipient mouse, lines are the median, error bar show min to max. Data are pooled from at least two repeats with $n \geq 3$ mice/group.

ns, not significant. Mann-Whitney test for statistical significance.

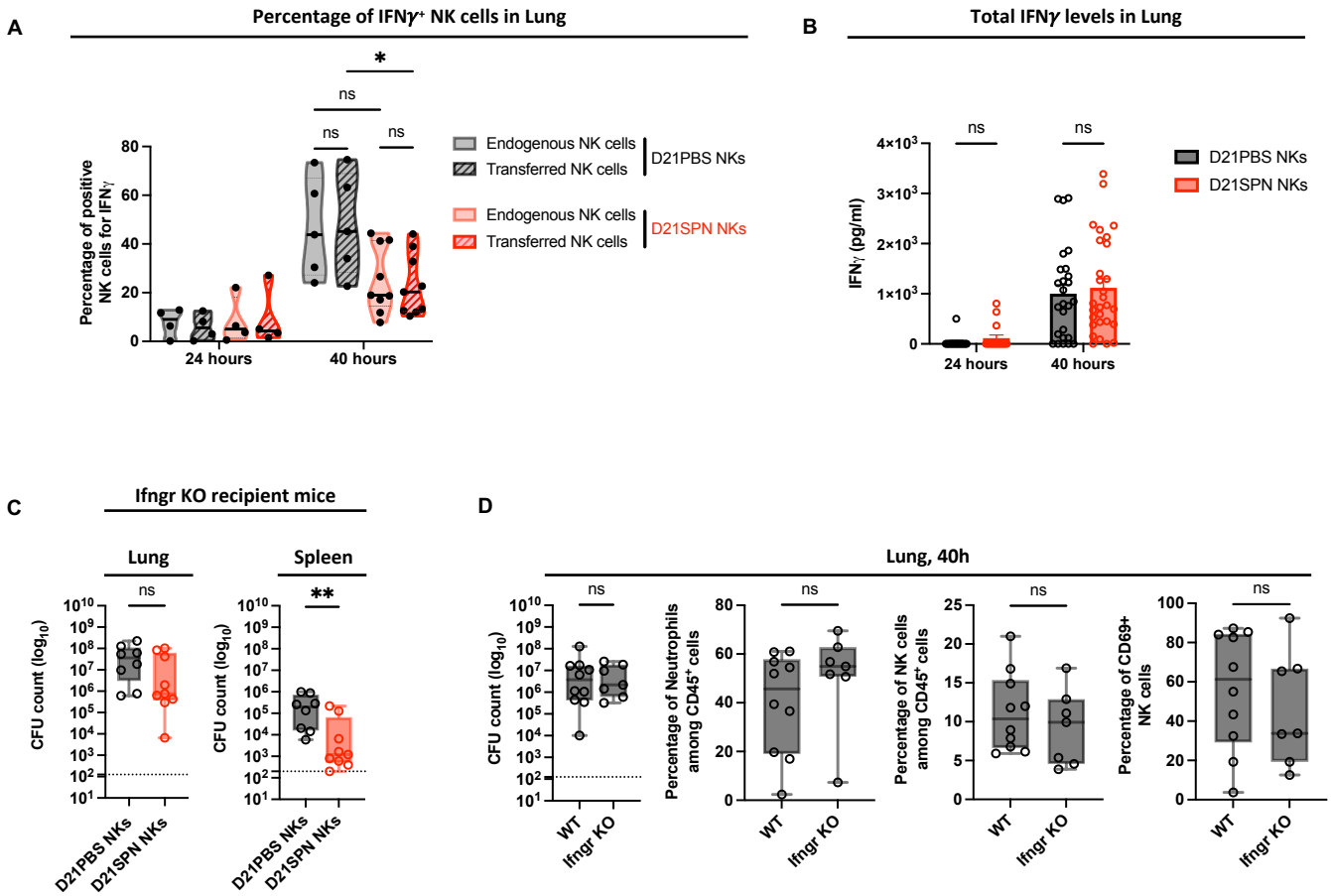

Figure 4: Protection of mice mediated by memory NK cells is IFNγ independent

(A-B) Mouse infections are carried out as in the scheme in Figure 3A. Organs were collected at 24h and 40h post-infection for flow cytometry analysis and ELISA assays.
(A) Flow cytometry analysis of IFNγ expression in CD45.1$^+$ endogenous NK cells and CD45.2$^+$ transferred NK cells (hatched) into both mice having received D21PBS NK cells (black) and mice having received D21SPN NK cells (red). Violin plot where each dot represents an individual mouse, lines are the median. Data are pooled from two repeats with n $\geq$ 2 mice/group.
(B) IFNγ ELISA assays of lung supernatants from infected mice having received either D21PBS NKs (black) or D21SPN NKs (red) at 24h and 40h post-infection. Bars are the mean of at least four experiments with n $\geq$ 4 mice/group, each dot represents an individual mouse and error bars are the standard error of the mean (SEM).
(C) Mouse infections are carried out as in the scheme in Figure 3A, with the exception that WT mice were used as donor mice and Ifngr KO mice as recipient mice. Bacterial counts at 40h post-infection in the lungs and spleen of Ifngr KO mice having received D21PBS WT NK cells (black symbols) or D21SPN WT NK cells (red symbols). Box plots where each dot represents an individual mouse, lines are the mean, error bars show min to max and dotted lines represent limit of detection. Data are pooled from two repeats with n $\geq$ 4 mice/group.
(D) WT and Ifngr KO mice were intranasally infected with a lethal dose of *S. pneumoniae* (1.10^7 CFU). Lungs were collected at 40h post-infection for CFU counts and flow cytometry analysis. Percentages of neutrophils (Ly6G$^+$ CD11b$^+$), NK cells (NK1.1$^+$ CD3$^-$) and CD69$^+$ NK cells. Box plots where each dot represents an individual mouse, lines are the mean, error bars show min to max and dotted lines represent limit of detection. Data are pooled from two repeats with n $\geq$ 3 mice/group
ns, not significant. * $p < 0.05$, ** $p < 0.01$. 2way ANOVA **(A,B)** and Mann-Whitney **(C,D)** tests for statistical significance.

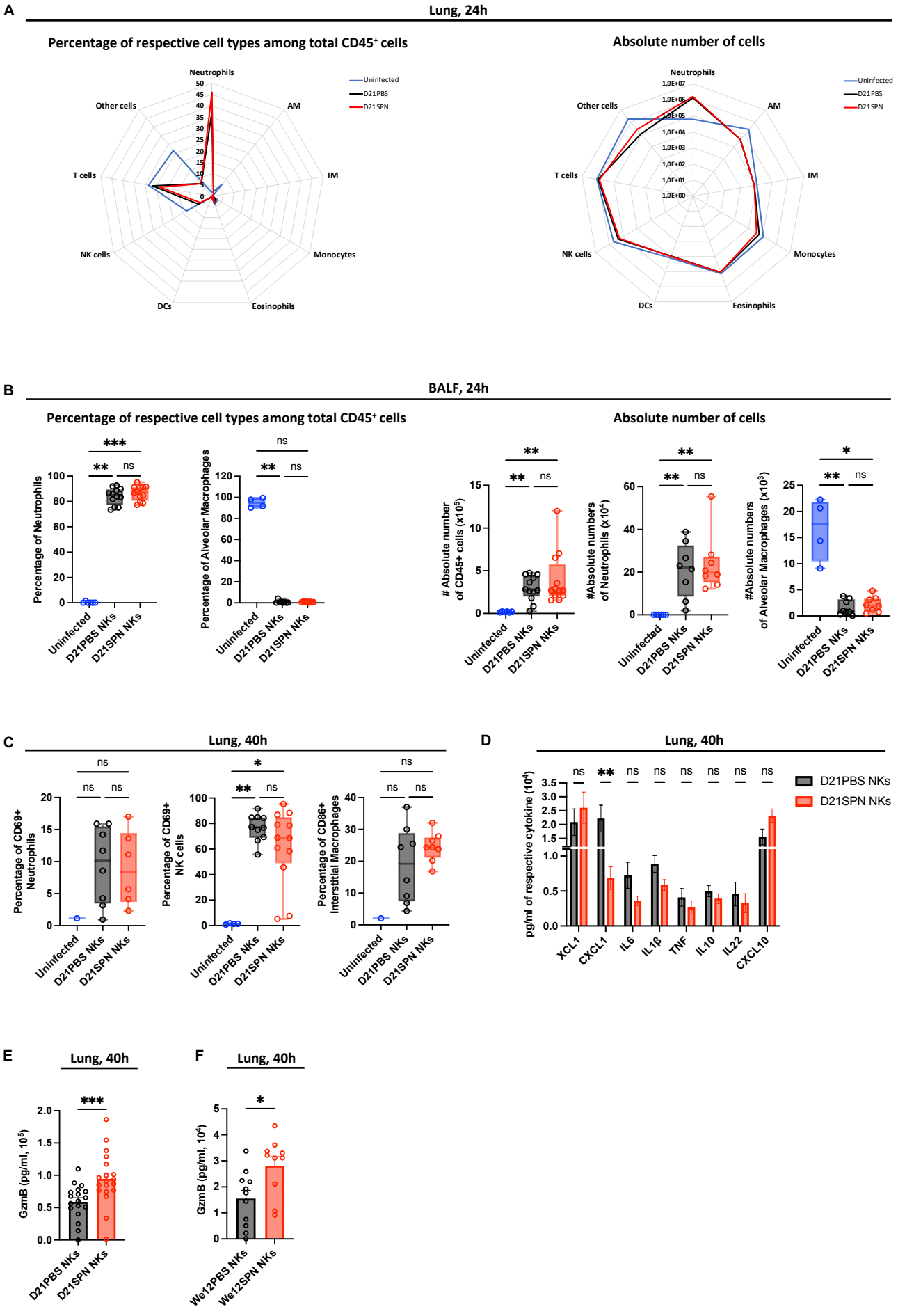
A
Lung, 24h
Percentage of respective cell types among total CD45⁺ cells
Absolute number of cells
Neutrophils
AM
IM
Monocytes
Eosinophils
DCs
NK cells
T cells
Other cells
Uninfected
D21PBS
D21SPN
B
BALF, 24h
Percentage of respective cell types among total CD45⁺ cells
Absolute number of cells
Percentage of Neutrophils
Percentage of Alveolar Macrophages
Absolute number of CD45+ cells (x10⁵)
#Absolute numbers of Neutrophils (x10⁴)
#Absolute numbers of Alveolar Macrophages (x10³)
Uninfected
D21PBS NKs
D21SPN NKs
C
Lung, 40h
Percentage of CD69+ Neutrophils
Percentage of CD69+ NK cells
Percentage of CD86+ Interstitial Macrophages
D
Lung, 40h
pg/ml of respective cytokine (10⁴)
XCL1
CXCL1
IL6
IL1β
TNF
IL10
IL22
CXCL10
D21PBS NKs
D21SPN NKs
E
Lung, 40h
GzmB (pg/ml, 10⁵)
F
Lung, 40h
GzmB (pg/ml, 10⁴)
We12PBS NKs
We12SPN NKs

Figure 5: Protection of mice appears to be an intrinsic NK cell property

Mouse infections are carried out as in the scheme in Figure 3A. Organs were collected at 24h and 40h post-infection for flow cytometry analysis, ELISA assays and CFU counts.

(A) Cellular infiltrate analysis in the lungs at 24h post-infection. Percentage of respective cell types among $CD45^+$ cells (**left panel**) and absolute number of cells for each cell type (**right panel**): neutrophils ($Ly6G^+$ $CD11b^+$), alveolar macrophages (AM) ($Ly6G^-$ $SiglecF^+$ $CD64^+$ $CD11b^-$), interstitial macrophages (IM) ($Ly6G^-$ $SiglecF^-$ $CD11b^{high}$ $MHCII^+$ $CD64^+$ $CD24^-$), monocytes ($Ly6G^-$ $SiglecF^-$ $CD11b^{high}$ $MHCII^-$), eosinophils ($Ly6G^-$ $SiglecF^+$ $CD11b^+$), dendritic cells (DCs) ($CD103^+$ DCs : $Ly6G^-$ $SiglecF^-$ $CD11b^{low}$ $CD103^+$ $CD24^+$ + $CD11b^+$ DCs : $Ly6G^-$ $SiglecF^-$ $CD11b^{high}$ $MHCII^+$ $CD64^-$ $CD24^+$), NK cells ($NK1.1^+$ $CD3^-$), T cells ($NK1.1^-$ $CD3^+$). Radar plots with each value representing the geometric mean of three repeats with n = 4 mice. The blue line for uninfected mice, black line for mice having received D21PBS NKs and red line for mice having received D21SPN NKs.

(B) Cellular infiltrate analysis in the bronchio-alveolar lavage fluid (BALF) at 24h post-infection. Percentage of respective cell types among $CD45^+$ cells (**left panel**) and absolute number of cells for each cell type (**right panel**): neutrophils ($Ly6G^+$ $CD11b^+$), alveolar macrophages ($SiglecF^+$ $CD64^+$ $CD11b^-$). Box plots where each dot represents an individual mouse (blue dots for uninfected mice, black dots for mice having received D21PBS NKs, red dots for mice having received D21SPN NKs), lines are the median, error bar show min to max. Date are pooled from at least two repeats with $n \geq 2$ mice/group.

(C) Cellular activation analysis in the lung at 40h post-infection. Percentages of $CD69^+$ neutrophils, $CD69^+$ NK cells and $CD86^+$ interstitial macrophages. Box plots where each dot represents an individual mouse (the blue dots are for uninfected mice, black dots for mice having received D21PBS NKs, red dots for mice having received D21SPN NKs), lines are the median, error bar show min to max. Data are pooled from two repeats with $n \geq 1$ mice/group.

(D) ELISA assays of lung supernatants from infected mice at 40h post-infection. Bars are the mean of at least 3 experiments with $n \geq 3$ mice/group, error bars are the standard error of the mean (SEM).

(E-F) At 40h post-infection, lung supernatants of mice having received either D21PBS NKs (black) or D21SPN NKs (red) **(C) -** either We12PBS NKs (black) or We12SPN NKs (red) **(D)** were collected to perform Granzyme B ELISA assays. Bars are the mean of at least 3 experiments with $n \geq 3$ mice/group, each dot represents an individual mouse and error bars are the standard error of the mean (SEM).

ns, not significant. * $p < 0.05$, ** $p < 0.01$, *** $p < 0.001$. Kruskal-Wallis **(A,B,C)**, 2way ANOVA **(D)** and Mann-Whitney **(E,F)** tests for statistical significance.

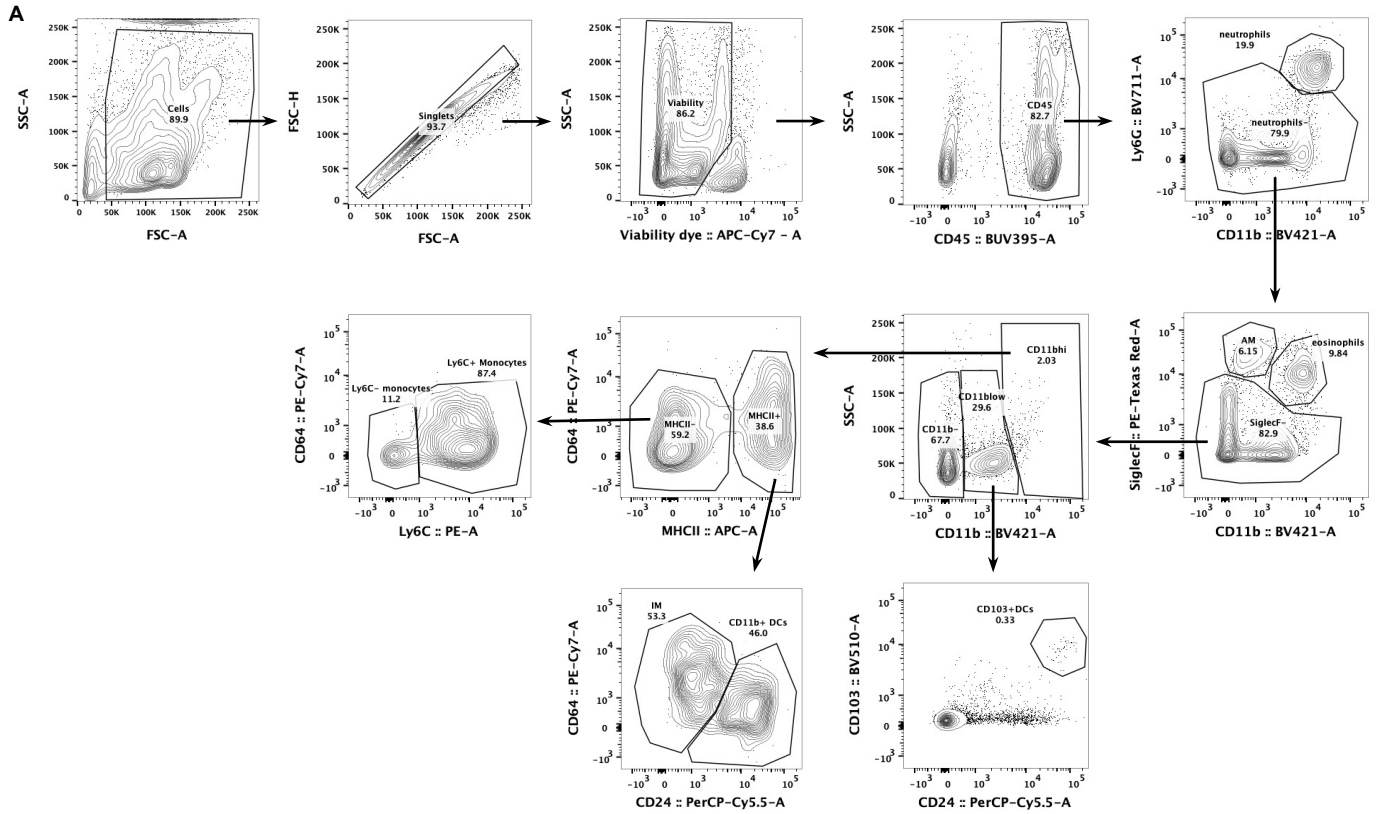
A
SSC-A
FSC-A
Cells
89.9
FSC-H
Singlets
93.7
Viability
86.2
Viability dye :: APC-Cy7 - A
CD45
82.7
CD45 :: BUV395-A
Ly6G :: BV711-A
neutrophils
19.9
neutrophils
79.9
CD11b :: BV421-A
SiglecF :: PE-Texas Red-A
AM
6.15
eosinophils
9.84
SiglecF+
82.9
CD11bhi
2.03
CD11blow
29.6
CD11b-
67.7
CD64 :: PE-Cy7-A
MHCII-
59.2
MHCII+
38.6
MHCII :: APC-A
Ly6C+ Monocytes
87.4
Ly6C- monocytes
11.2
Ly6C :: PE-A
IM
53.3
CD11b+ DCs
46.0
CD24 :: PerCP-Cy5.5-A
CD103+DCs
0.33
CD103 :: BV510-A

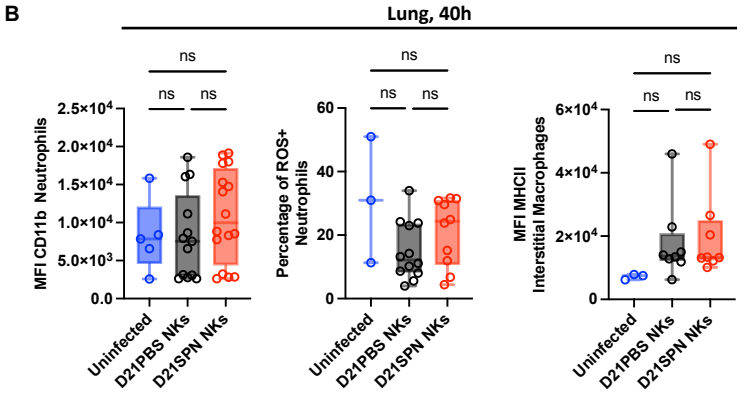
B
Lung, 40h
MFI CD11b Neutrophils
Percentage of ROS+ Neutrophils
MFI MHCII Interstitial Macrophages
ns
Uninfected
D21PBS NKs
D21SPN NKs

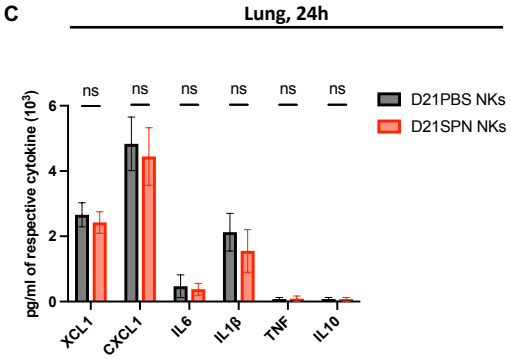
C
Lung, 24h
pg/ml of respective cytokine (10³)
XCL1
CXCL1
IL6
IL1β
TNF
IL10
D21PBS NKs
D21SPN NKs

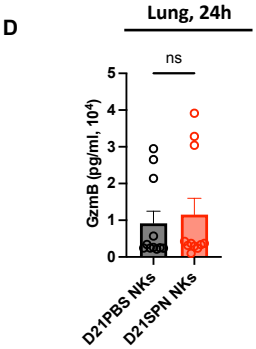
D
Lung, 24h
GzmB (pg/ml, 10⁴)
D21PBS NKs
D21SPN NKs

Figure S4

Mouse infections are carried out as in the scheme in Figure 3A. Organs were collected at 24h and 40h post-infection for flow cytometry analysis and ELISA assays.

(A) Gating strategy used to identify myeloid-cell subsets in the lungs at 24h post-infection, adapted from Misharin *et al*. 2013. After the exclusion of debris, doublets and dead cells, immune cells were identified by CD45 staining. Neutrophils, alveolar macrophages and eosinophils are defined with the following specific markers respectively: $Ly6G^{+}$ $CD11b^{+}$, $SiglecF^{+}$ $CD11b^{-}$, $SiglecF^{+}$ $CD11b^{+}$. Gating on $CD11b^{high}$ was used to distinguish myeloid cells from lymphoid cells with the exception of $CD103^{+}$ dendritic cells that are defined as $CD11b^{low}$ $CD103^{+}$ $CD24^{+}$ cells. In $CD11b^{high}$ subset, gating on $MHCII^{+}$ cells allow to identify interstitial macrophages as $MHCII^{+}$ $CD64^{+}$ $CD24^{-}$ cells and $CD11b^{+}$ dendritic cells as $MHCII^{+}$ $CD64^{-}$ $CD24^{+}$ cells. On the contrary, $CD11b^{high}$ $MHCII^{-}$ cells are monocytes/immature macrophages that can have different maturation states based on Ly6C marker.

(B) Cellular activation analysis in the lungs at 40h post-infection. Intensity of CD11b expression in neutrophils (MFI), percentage of ROS^{+} neutrophils and intensity of MHCII expression in interstitial macrophages (MFI). Box plots with each dot representing individual mice (blue dots for uninfected mice, black dots for mice having received D21PBS NKs, red dots for mice having received D21SPN NKs), lines are the median, error bar show min to max. Data are pooled from two repeats with $n \geq 1$ mice/group.

(C) ELISA assays of lung supernatants from infected mice having received either D21PBS NKs (black) or D21SPN NKs (red) at 24h post-infection. Bars are the mean of at least 3 experiments with $n \geq 3$ mice/group, error bars are the standard error of the mean (SEM).

(D) Granzyme B ELISA assays of lung supernatants from infected mice having received either D21PBS NKs (black) or D21SPN NKs (red) at 24h post-infection. Bars are the mean of at least 3 experiments with $n \geq 3$ mice/group, error bars are the standard error of the mean (SEM).

ns, not significant.. Kruskal-Wallis **(B),** 2way ANOVA **(C)** and Mann-Whitney **(D)** tests for statistical significance.

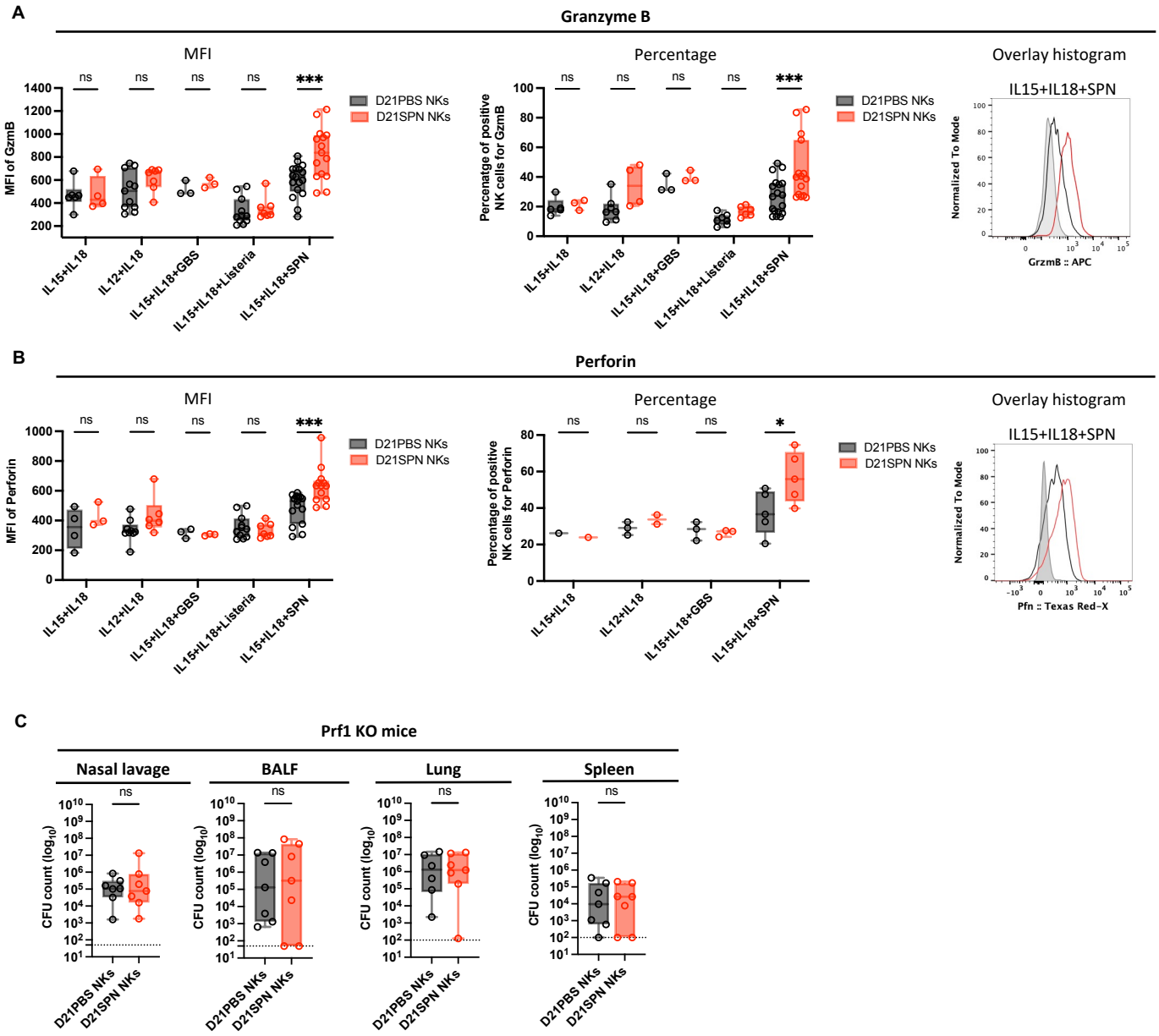

Figure 6: Cytotoxic proteins are upregulated by memory NK cells and and important for protection of mice

(A-B) C57BL/6 mice were intranasally injected with either PBS (black symbols) or sub-lethal dose of *S. pneumoniae* (SPN, red symbols, 5.10^5 CFU) for two consecutive days. After 21 days, NK cells were highly purified from spleens of D21PBS or D21SPN mice (98% of purity) and stimulated *in vitro* with cytokines (IL-15 at 2 ng/ml, IL-18 at 1,5 ng/ml, IL-12 at 1,25 ng/ml) and formaldehyde inactivated bacteria (MOI 20) for 24 hours.
SPN : *S. pneumoniae*, GBS : *S. agalactiae,* Listeria : *L. monocytogenes*.
(A) Intensity of Granzyme B expression in NK cells (MFI, **left panel**), percentage of Granzyme B^+ NK cells (**middle panel**), representative overlay histogram upon IL-15+IL-18+SPN stimulation (**right panel**, gray represents isotype control). Box plots where each dot represents a pool of mice from one experiment (black dots for D21PBS NKs, red dots for D21SPN NKs), line are median, error bar show min to max. Data are representative of at least one experiment with $n \geq 4$ pooled mice/group and $n \geq 3$ experimental replicates/group.
(B) Intensity of Perforin expression in NK cells (MFI, **left panel**), percentage of Perforin$^+$ NK cells (**middle panel**), representative overlay histogram upon IL-15+IL-18+SPN stimulation (**right panel**, gray represents isotype control). Box plots where each dot represents a pool of mice from one experiment (black dots for D21PBS NKs, red dots for D21SPN NKs), line are median, error bar show min to max. Data are representative of at least one experiment with $n \geq 4$ pooled mice/group and $n \geq 3$ experimental replicates/group.
(C) Mouse infections are carried out as in the scheme in Figure 3A, with the exception that Prf1 KO mice were used as both donor and recipient mice. Bacterial counts at 40h post-infection in the nasal lavage, bronchio-alveolar lavage fluid (BALF), lungs and spleen of Prf1 KO mice having received D21PBS Prf1 KO NK cells (black symbols) or D21SPN Prf1 KO NK cells (red symbols). Box plots where each dot represents an individual mouse, lines are the mean, error bars show min to max and dotted lines represent limit of detection. Data are pooled from two repeats with $n \geq 3$ mice/group.
ns, not significant. * $p < 0.05$, *** $p < 0.001$. 2way ANOVA **(A,B)** and Mann-Whitney **(C)** tests for statistical significance.

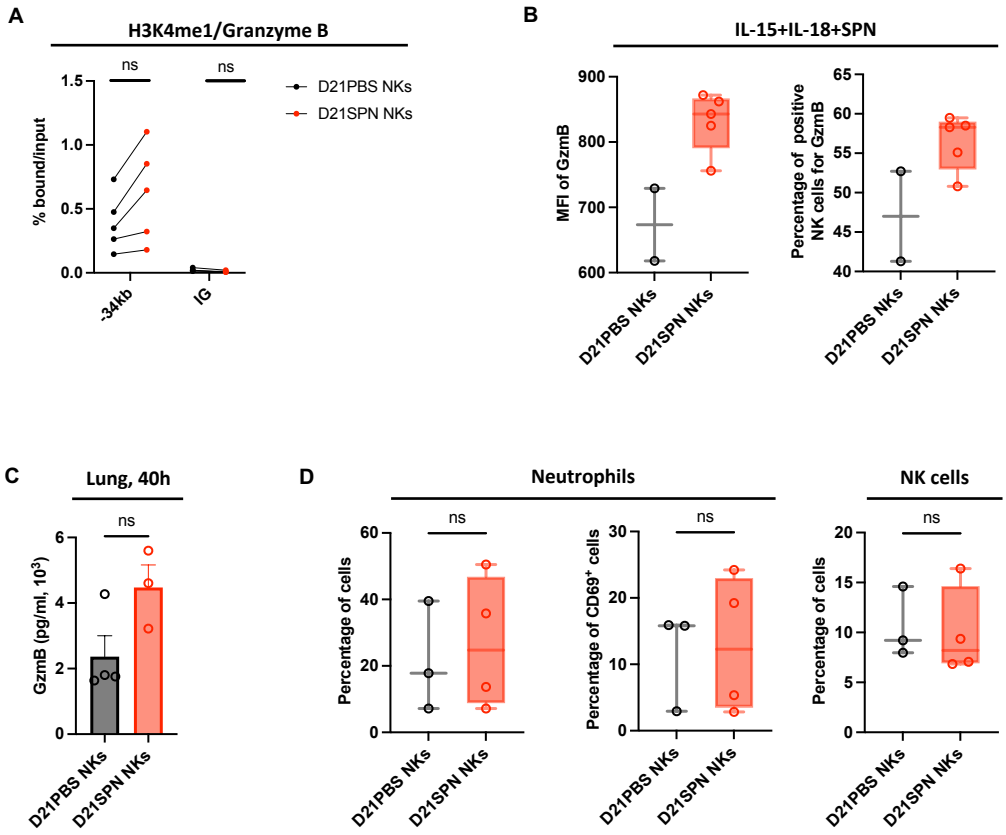

Figure S5

(A) Mouse infections are carried out as in the scheme in Figure 1A. NK cells were isolated from spleens of mice previously infected with *S. pneumoniae* (red bars, D21SPN NKs) or not (black bars, D21PBS NKs). Highly purified NK cells were fixed, and chromatin was extracted and sheared. ChIP for H3K4me1 were performed and resulting positive fractions of the chromatin were amplified using PCR for the indicated targets. Enrichment percentage for H3K4me1 pull-down on -34kb upstream the *gzmb* gene and intergenic regions (IG) in NK cells from D21PBS and D21SPN mice. Data are representative of at least three experiments with n ≥ 4 mice/group.
(B) Mouse infections and *in vitro* experiments are carried out as in the scheme in Figure 1A, with the exception that Prf1 KO mice were used. Purified D21PBS (black) or D21SPN (red) Prf1 KO NK cells were stimulated *in vitro* with cytokines (IL-15 at 2 ng/ml and IL-18 at 1,5 ng/ml) and formaldehyde inactivated *S. pneumoniae* (SPN, MOI 20) for 24 hours. Intensity of Granzyme B expression in NK cells (MFI, **left panel**) and percentage of Granzyme B^+ NK cells (**right panel**) upon *in vitro* stimulation. Box plots where each dot represents a pool of mice from one experiment, line are median, error bar show min to max. Data are representative of one experiment with n = 4 pooled mice/group and n ≥ 2 experimental replicates/group.
(C-D) Mouse infections and *in vivo* transfers are carried out as in the scheme in Figure 3A, with the exception that Prf1 KO mice were used as both donor and recipient mice.
(C) Granzyme B ELISA experiment of lung supernatants from infected mice at 40h post-infection, having received either D21PBS (black) or D21SPN (red) Prf1 KO NK cells. Dots represent individual mice, bars are the mean and error bars are the standard error of the mean (SEM). Data are representative of one experiment with n ≥ 3 mice/group.
(D) Percentages of neutrophils, $CD69^+$ neutrophils and NK cells in the lungs of Prf1 KO recipient mice having received either D21PBS (black) or D21SPN (red) Prf1 KO NK cells. Box plots with each dot representing individual mice, lines are the median, error bar show min to max. Data are representative of one experiment with n ≥ 3 mice/group.
ns, not significant. Mann-Whitney tests for statistical significance.